Paterson AEM Survey: Inversion Report

GEOSCIENCE AUSTRALIA
GEOCAT 70297

by

D.K. Hutchinson, M.T. Costelloe, I.C. Roach and C. Sorensen

Australian Government
Geoscience Australia

APPLYING GEOSCIENCE TO AUSTRALIA'S
MOST IMPORTANT CHALLENGES

Department of Resources, Energy and Tourism
Minister for Resources and Energy: The Hon. Martin Ferguson, AM MP
Secretary: Mr Drew Clarke

Geoscience Australia
Chief Executive Officer: Dr Chris Pigram

© Commonwealth of Australia, 2010

This work is copyright. Apart from any fair dealings for the purpose of study, research, criticism, or review, as permitted under the *Copyright Act 1968*, no part may be reproduced by any process without written permission. Copyright is the responsibility of the Chief Executive Officer, Geoscience Australia. Requests and enquiries should be directed to the **Chief Executive Officer, Geoscience Australia, GPO Box 378 Canberra ACT 2601**.

Geoscience Australia has tried to make the information in this product as accurate as possible. However, it does not guarantee that the information is totally accurate or complete. Therefore, you should not solely rely on this information when making a commercial decision.

GeoCat # 70297

Bibliographic reference: D.K. Hutchinson, M.T. Costelloe, I.C. Roach and C. Sorenson 2010. Paterson AEM Survey: Inversion Report. Geoscience Australia internal report.

Contents

Executive Summary **1**
1 Introduction **2**
1.1 Survey purpose 2
1.2 Previously released data 3
1.3 TEMPEST AEM system 4
1.4 Background on the GA-LEI inversion 5
2 GA-LEI Inversions **7**
2.1 Description 7
2.2 Conductivity Reference Model 9
3 GA-LEI inversion products **10**
3.1 Depth of Investigation 10
3.2 Grids 11
3.2.1 Gridding parameters 12
3.2.2 AEM Go Map 12
3.2.3 Depth Slices 13
3.2.4 Elevation slices 14
3.3 Sections 16
3.3.1 Georeferenced jpegs 16
3.3.2 GA-LEI multiplots 17
3.4 Discrete conductors 18
4 Validation **21**
4.1.1 Conductivity Logging 21
5 Summary **27**
6 Acknowledgements **28**
7 References **29**
Appendix 1 Accompanying DVD **31**
Appendix 2 Inversion control file **33**
Appendix 3 Conductivity data header information **36**
Appendix 4 Technical specifications of map projections **37**
Appendix 5 Conductivity logging **38**
A5.1 Method 38
A5.2 Results 39
A5.3 Field sheets 49

Figures

Figure 1: Paterson Survey boundary locations. Internal survey boundary locations with a prefix N represent infill companies for North Paterson. Internal Survey boundary locations with a prefix S represent infill companies for South Paterson. The 200 m line spaced-data highlighted in N5 is GA-funded.....3
Figure 2: Schematic diagram of 1D vertically smooth layered earth model used in the GA-LEI. The thickness of each layer (t_n) is fixed , but the conductivity (σ_n) is not fixed and can vary between layers. From Brodie and Fisher (2008). 8
Figure 3: Sample conductivity depth sections comparing the results of inversions using reference models of (a) 0.04 S/m and (b) 0.004 S/m. The black line marks the depth of investigation (DOI) in each case. Above the DOI, the results are similar for both inversions, whereas below the DOI the conductivity differs according to the reference model value. 11
Figure 4: The DOI grid. 13
Figure 5: A selection of depth slices showing a) 0-5 m, b) 30-40 m, c) 100-150 m and d) 200-250 m. Data falling below the DOI have been masked out, and appear white. 14
Figure 6: Selection of elevation slices, showing a) 0-10 m above sea level (a.s.l.), (b) 100-110 m a.s.l., (c) 200-210 m a.s.l. and (d) 300-310 m a.s.l.....15
Figure 7: Georeferenced jpeg for line 10000. Elevation above sea level is in metres and is labelled on the left hand side of each plot. The horizontal scale is provided in the accompanying .jgw world file.....16
Figure 8: Colour bar for georeferenced jpegs. One colour bar is provided to reference to all lines. .17
Figure 9: GA-LEI multiplot for line 10000.....18
Figure 10: A FAS multiplot for line 20641 from the Paterson South survey area.....19
Figure 11: Sub-section of the multiplot for line 20641 highlighting the discrete conductor response in the X and Z component windows. 20
Figure 12: A comparison between EMFlow and GA-LEI conductivity sections for line 20641. a). Subsection of the GA-LEI inversion for line 20641 highlighting the discrete conductor response. b). Subsection of the FAS EMFlow CDI for line 20641. Please note the vertical exaggeration differs between plots. 20
Figure 13: The location of the boreholes plotted over conductance from 0-200 m.. 23
Figure 14: Conductivity logs compared to GA-LEI results.....24
Figure 15: Conductivity logs compared to GA-LEI results (continued).....25
Figure 16: Conductivity logs compared to GA-LEI results (continued).....26
Figure 17: Conductivity logs compared to GA-LEI results (continued).....27
Figure A1: The principle of operation of inductive conductivity borehole logging tool, from McNeill (1990). 38
Figure A2: Comparison of logs from the repeat hole, from the beginning and end of field trip. Run1 and Run2 were acquired at the beginning of the trip, and Repeat1 and Repeat2 were acquired at the end of the field trip.....40
Figure A3: The 14 publicly available conductivity logs, showing the repeat passes acquired for each log. 48

Tables

Table 1: TEMPEST AEM system specifications from Lane *et al.* (2000).....5
Table 2: GA-LEI model layer thicknesses and depths from surface.....8
Table 3: JPEG world file contents for line 10000.....16
Table 4: Coordinates (MGA94 Zone 51) and depths of the 19 boreholes.....22
Table A1: Field sheets acquired for conductivity logs.....49

Executive Summary

Airborne Electromagnetic data are being acquired by Geoscience Australia in areas considered to have potential for uranium or thorium mineralisation under the Australian Government's Onshore Energy Security Program (OESP). The surveys have been managed and interpreted by Geoscience Australia's Airborne Electromagnetic Acquisition and Interpretation project. In contrast to industry style deposit scale investigations, these surveys are designed to reveal new geological information at regional scale. The Paterson airborne electromagnetic data were acquired at line spacings of between one and six kilometres, a total of 28 200 line km and covers an area of 47 600 km^2.

The outcomes of the Paterson AEM survey include mapping of subsurface geological features that are associated with unconformity-related, sandstone-hosted and palaeovalley-hosted uranium mineralisation. The data are also capable of interpretation for other commodities including metals and potable water as well as for landscape evolution studies. The improved understanding of the regional geology resulting from the Paterson survey results will be of considerable benefit to mining and mineral exploration companies.

Phase-1 data, that is, contractor quality-controlled and quality-assessed data, were released during 2009. Phase-2 data, that is Geoscience Australia layered earth inversion (GA-LEI) data and derived products, are included in this data release. The data and products described in this report are contained on the accompanying DVD.

The main products from the AEM survey are conductivity depth slices and sections, conductance grids and an AEM Depth of Investigation grid. The data is provided in formats which can be viewed on most computers systems. They include, JPEG (.jpg) with associated world files for easy use in geographic information system (GIS) packages, ER Mapper grids (.ers), ESRI shape files (.shp) of the flight path, and point-located ASCII data with relevant metadata for derived products.

1 Introduction

1.1 Survey purpose

Airborne Electromagnetic (AEM) surveys are commonly used to map the electrical conductivity of the subsurface over large spatial areas. As an AEM system flies over the ground it carries a transmitter loop through which a time-varying current is passed, thereby inducing eddy (secondary) currents to flow in any electrically conductive subsurface material. These eddy currents may be detected via the voltage that they induce in receiver coils that are towed by the aircraft. Since the amount of current that flows in the subsurface is related to its conductivity, analysis of the received signals allows estimates of the conductivity to be made. The depth to which the signals can be used to map conductivity depends on the system configuration and the subsurface conductivity (Smith, 2001a, Lane *et al.*, 2004b).

The Paterson AEM survey was the first of three regional AEM surveys undertaken as part of the Onshore Energy Security Program (OESP) at Geoscience Australia (GA). The survey in the Paterson Province of Western Australia (**Figure 1**) covered sections of the Anketell, Balfour Downs, Gunanya, Nullagine, Paterson Range, Rudall, Runton, Tabletop and Yarrie 1:250 000 map sheets (Costelloe *et al*., 2007). Fugro Airborne Surveys (FAS) were contracted to fly the surveys using its TEMPEST system during 2007-2008. A total of 28 200 line kilometres of data were acquired along broadly spaced flight lines (up to 6 km spacing). The survey was conducted with the transmitter loop nominally at 120 m above ground level.

The basic data from the survey, herein referred to as Phase-1 data, were publicly released in 2009 (*cf.* Section 1.2). This Phase-2 report presents results of layered earth inversions and other products derived from the dataset. The Phase-2 report contains discussions on the inversion process, limitations of the data in the Phase-1 release and how the layered earth inversion products add value to the Paterson AEM survey data. The estimated conductivity data are presented in several forms of cross-sections, elevation slices, depth slices, as well as in grids of total conductance.

The survey results have improved the understanding of the area's geology and mineral potential by mapping the conductivities of different geological and hydrogeological units under cover. The dataset contributes to interpretations regarding the presence of graphitic units in the Rudall Complex, the location of major structures and the extent of Permian and Cenozoic palaeovalleys and other Phanerozoic regolith features. A detailed interpretation of the data is included in the report *"Geological and energy implications of the Paterson Province Airborne electromagnetic (AEM) survey, Western Australia"* (Roach, 2010) *GA Record 2010/12***.**

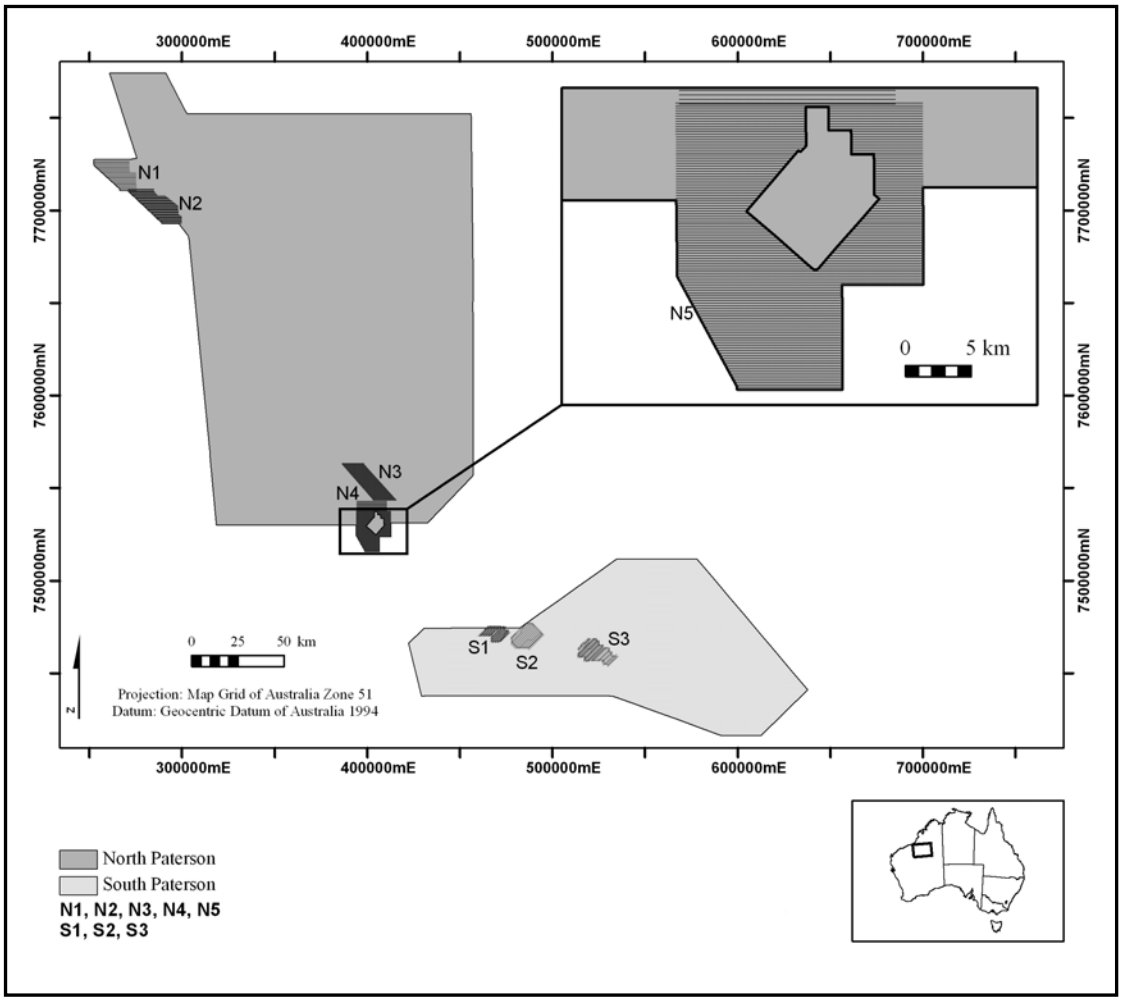

***Figure 1**: Paterson Survey boundary locations. Internal survey boundary locations with a prefix N represent infill companies for North Paterson. Internal survey boundary locations with a prefix S represent infill companies for South Paterson. The 200 m line spaced-data highlighted in N5 is GA-funded.*

1.2 Previously released data

Due to industry delivery requirements, the survey was flown in two separate blocks, named Paterson South and Paterson North, which are shown on the locality map (**Figure 1**). Internal to these two main survey blocks are eight sub-areas of infill flying that were funded by exploration companies. The flight lines that were funded by these companies were not included in the Phase-1 data release as, under the terms of the funding agreement, there was a moratorium on the data until April 2010.

The Phase-1 data release included contractor supplied data that had been quality controlled and assured by GA. The GA-funded portion of the Paterson South contractor supplied data was released on 4th March 2009 and the Paterson North data were released on 17th April 2009.

The Phase-1 data release contained:

1. Survey operations and processing report;
2. Point located electromagnetic response data without correction to a standard geometry;
3. Point located electromagnetic response data with correction to a standard geometry;
4. Point located conductivity depth image data derived using the program EMFlow;

5. Gridded electromagnetic response and CDI data; and
6. Graphical multiplots profiles showing electromagnetic, CDI and ancillary data for each line.

These data are available from the GA Sales Centre and are also available by free download from the GA website. Downloads are available through the links below:

1. Paterson South Phase-1 data and processing report;
https://www.ga.gov.au/products/servlet/controller?event=GEOCAT_DETAILS&catno=68430.

2. Paterson North Phase-1 data and processing report;
https://www.ga.gov.au/products/servlet/controller?event=GEOCAT_DETAILS&catno=68761.

3. Entire Paterson Phase-1 data including the infill data funded by private companies:
https://www.ga.gov.au/products/servlet/controller?event=GEOCAT_DETAILS&catno=70312.

Phase-1 data included Conductivity Depth Images (CDI) generated by FAS using the software EMFlow. The EMFlow CDI program is an industry standard method of deriving conductivity estimates from AEM surveys. The conductivity estimates that are contained in the Phase-2 data, and reported on herein, have been produced by the GA-LEI inversion algorithm that has been developed at GA.

1.3 TEMPEST AEM system

The Paterson survey was flown with Fugro Airborne Surveys' TEMPEST AEM System (Lane *et al.*, 2000) which was installed on the aircraft with registration VH-TEM. A summary of the system configuration used in the Paterson survey is provided in **Table 1**. The acquisition and processing of the Paterson North and Paterson South survey data is detailed in Lawrence and Stenning (2007a) and Lawrence and Stenning (2007b) respectively.

TEMPEST is a fixed-wing time-domain system. It employs an approximate square-wave 50% duty cycle current waveform with a base frequency of 25 Hz. The current is transmitted through a single turn transmitter (TX) loop draped around the nose, wings and tail of the aircraft. The survey was flown with the TX loop at 122.4 m above ground level on average.

The receiver (RX) coils were housed in a 'bird' that was towed at approximately 120 m behind and 35 m below the aircraft. The RX consists of three orthogonal coils that sense the rate of change of the magnetic field (dB/dt) flux threading each coil. The axes of the three coils are nominally aligned in the horizontal flight line direction (X-component), horizontal direction perpendicular to the flight line (Y-component), and vertical directions (Z-component). However, only the X and Z-components are recorded and processed at full resolution and thus available for interpretation.

The TX height and the orientations and relative separations of the TX and RX are also known as the system geometry. The system geometry continuously varies as the aircraft moves along each flight line. The TEMPEST instrumentation includes a GPS unit to the aircraft's position, radar and laser altimeters to measure its height above ground level, and gyroscopes to measure its roll, pitch and yaw angles (i.e. its orientation). The relative separations of the TX and RX and the orientation of the RX are not measured by the system because of the logistical difficulty in doing so.

Since the system geometry affects the measured response, it must be used for (input into) quantitative forward modelling of the system response, and hence estimation of subsurface conductivity from the recorded data. Therefore, in the data processing the unmeasured elements of the system geometry need to be estimated. For the TEMPEST system this involves separation of the measured total field response into its primary field (due to direct coupling between TX and RX) and secondary field (due to eddy currents induced in the ground) components. This requires an assumption to be made about the unknown subsurface conductivity, which typically is that the

subsurface is resistive at depth. Once separated into primary and secondary components, the horizontal and vertical offsets between the TX and RX can be analytically determined from the primary field if it is assumed that the receiver bird is orientated with zero roll, pitch and yaw. It is these estimated and assumed values of system geometry that are taken to be the real values in standard algorithms for estimating subsurface conductivity from the measured data.

Table 1: TEMPEST AEM system specifications from Lane *et al.* (2000).

Base frequency	25 Hz
Transmitter area	221 m^2 (VH-TEM)
Transmitter turns	1
Waveform	Square
Duty cycle	50%
Transmitter pulse width	10 ms
Transmitter off time	10 ms
Peak current	280 A (VH-TEM)
Peak moment	61880 Am^2 (VH-TEM)
Average moment	30940 Am^2 (VH-TEM)
Sample rate	75 kHz on X and Z
Sample interval	13.333 microseconds
Samples per half cycle	1500
System bandwidth	25 Hz to 37.5 kHz
Tx Loop Flying height nominal	121.1 m (subject to safety considerations)
Tx Loop Flying height average	122.4 (VH-TEM)
EM sensor	Towed bird with 3 component dB/dt coils
Tx Rx horizontal separation average	120.1 (VH-TEM)
Tx Rx vertical separation average	34.5 (VH-TEM)
Tx Rx horizontal separation standard	120 m (geometry corrected standard)
Tx Rx vertical separation standard	35 m (geometry corrected standard)
Stacked data output interval	200 ms (~12 m)
Number of output windows	15
Window centre times	13 μs to 16.2 ms
Magnetometer	Stinger mounted caesium vapour
Magnetometer compensation	Fully digital
Magnetometer output interval	200 ms (~12 m)
Magnetometer resolution	0.001 nT
Typical noise level	0.2 nT
GPS cycle rate	1 second

1.4 Background on the GA-LEI inversion

Conversion of the non-linear electromagnetic response data into estimates of subsurface conductivity allows for much easier and more accurate integration with independent subsurface information and facilitates better interpretation. The conversion can use either approximate transformation methods or geophysical inversion, both of which produce model-dependent conductivity estimates.

The Phase-1 data release of Paterson data included conductivity predictions produced by FAS from the industry standard EMFlow algorithm (Macnae *et al.*,1998; Stolz and Macnae, 1998). EMFlow is a fast approximate transformation method based on the concept that the response of a quasi-layered earth can be approximately represented by a mirror image of the transmitter dipole that recedes below the surface and expands with delay-time. By determining the vertical depth distribution of the mirror image dipoles a quasi-layered estimate of the subsurface conductivity can be estimated.

Since the routine relies on the estimates of the system geometry that are made during the FAS data processing (*cf.* Section 1.3) the accuracy of the resultant conductivity estimates are dependent on the accuracy of the geometry estimates. Accordingly, the estimates tend to be biased towards producing results that are consistent with the assumptions made in the FAS data processing, namely a resistive

basement earth model. This bias can in turn create an overestimate of the conductivity near the surface, since the model must compensate for the lack of conductance at depth (Lane *et al*., 2004a; Brodie and Fisher, 2008).

A further problem is caused by the assumptions made in the system geometry estimation that the receiver is orientated in its nominal position (ie. with zero roll, pitch, and yaw). If the receiver is in fact rotated from its nominal position, which is generally the case, it may be impossible to simultaneously fit both the X- and Z-component data using the same subsurface conductivity distribution because the data are inconsistent with the information provided to the routine about the system geometry. For this reason it is often necessary to calculate the EMFlow estimates using just the X- or just the Z-component data. While this is possible a different conductivity model will result from each component.

These issues led to the development of the GA-LEI algorithm (Lane *et al*., 2004). In the GA-LEI inversion algorithm, the idea is to not rely on the primary field separation and hence geometry estimates made in the standard FAS data processing. Instead, the total field (primary plus secondary) field data are inverted directly. The inversion solves not only for a layered earth conductivity model, but it simultaneously solves for the horizontal and vertical separations between the TX and RX and the pitch of the receiver coils. By solving for the system geometry during the final inversion the method allows the information from both the X- and Z-components to be simultaneously fitted using a single common conductivity model. It prevents the assumptions made during the standard data processing from being automatically imposed onto the inversion results. Furthermore, if prior information exists about the electrical structure of the survey area, these can be included as specific constraints on the inversion results.

Previous work at GA, in which downhole conductivity log data were compared to conductivity estimates (Lane *et al*., 2004; Reid and Brodie 2006; Brodie and Fisher, 2008), has shown that improvements on the standard FAS EMFlow conductivity estimates can be made using the GA-LEI algorithm. The inversion products included in this data release have been derived with the GA-LEI algorithm. Chapter 2 of this report contains details of settings used in the GA-LEI for the Paterson survey. Chapter 3 of this report details the products derived from the GA-LEI inversions that are contained on the DVD compilation accompanying the report. For details on the product list and image enhancements refer to Appendix 1.

2 GA-LEI Inversions

2.1 Description

The GA-LEI is a 1D "sample-by-sample" inversion in which each of the airborne samples, that are acquired at approximately 12 m intervals along a flight line, are inverted independently of their neighbours. The inversion of each individual sample involves the estimation of a 1D layered earth conductivity structure that is consistent with the data. A 1D layered earth conductivity structure means that the earth is considered to be a series of horizontal layers stacked in layer-cake fashion. Each layer extends to infinity in the horizontal direction and the conductivity within each layer is constant. Once all samples are inverted they are compiled into a pseudo-3D model by 'stitching' the 1D model together.

A detailed technical description of the GA-LEI can be found in Lane *et al*. (2004) and Brodie and Fisher (2008). In this work the subsurface was parameterized with 30 layers whose thicknesses were chosen and remained fixed throughout the inversion (i.e. they were not solved for). The chosen layer thicknesses are shown in **Table 2**. We solved for the conductivity of each layer as shown in (**Figure 2**).

The inversion starts from a homogeneous conductivity model and iteratively approaches a solution that replicates the measured signal. The inversion is constrained to be vertically smooth and to be within specified bounds of a reference conductivity model. The aim of these smoothness and reference model constraints is to ensure that the model is as simple as possible, and complex structure is only permitted where necessary (see for example Constable *et al.*, 1987).

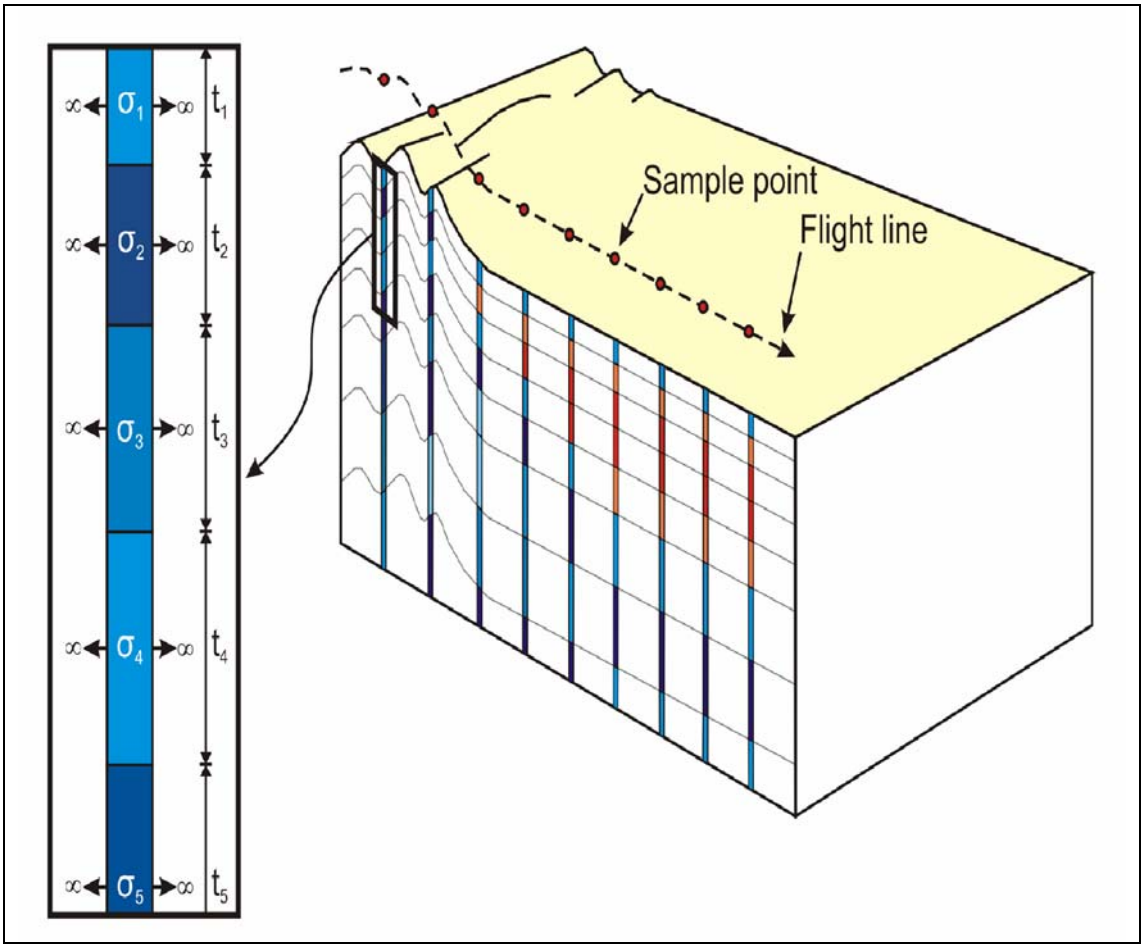

Figure 2: *Schematic diagram of 1D vertically smooth layered earth model used in the GA-LEI. The thickness of each layer (t_n) is fixed , but the conductivity (σ_n) is not fixed and can vary between layers. From Brodie and Fisher (2008).*

The layer thicknesses are specified as constraints in the model and gradually increase from 4 m in the top layer of the model up to approximately 60 m in the second deepest layer. The bottom layer itself is set to infinite thickness, representing a far-field response below the other layers. The thicknesses and depths of each layer used in the GA-LEI are shown in **Table 2**.

Table 2: GA-LEI model layer thicknesses and depths from surface.

LAYER NUMBER	THICKNESS (m)	DEPTH TO TOP (m)	DEPTH TO BOTTOM (m)
1	4.00	0.00	4.00
2	4.40	4.00	8.40
3	4.84	8.40	13.24
4	5.32	13.24	18.56
5	5.86	18.56	24.42
6	6.44	24.42	30.86
7	7.09	30.86	37.95
8	7.79	37.95	45.74
9	8.57	45.74	54.31
10	9.43	54.31	63.74
11	10.37	63.74	74.11

12	11.41	74.11	85.52
13	12.55	85.52	98.07
14	13.81	98.07	111.88
15	15.19	111.88	127.07
16	16.71	127.07	143.78
17	18.38	143.78	162.16
18	20.22	162.16	182.38
19	22.24	182.38	204.62
20	24.46	204.62	229.08
21	26.91	229.08	255.99
22	29.60	255.99	285.59
23	32.56	285.59	318.15
24	35.82	318.15	353.97
25	39.40	353.97	393.37
26	43.34	393.37	436.71
27	47.67	436.71	484.38
28	52.44	484.38	536.82
29	57.68	536.82	594.50
30	∞	594.50	∞

In the Paterson survey the TEMPEST data are recorded as a series of samples spaced 13.33 µs (75,000 Hz) apart. The system measures the total field response at the RX, which is the summation of the primary field (from the TX), and the secondary field (the ground response). The primary field depends on the system geometry, while the secondary field depends on both the system geometry and the ground conductivity. If the system geometry were measured in real time, the primary field could be deduced theoretically and subtracted from the total field measured by the RX. However, since the system geometry can only be partly measured, it can not be completely isolated. Thus the primary field, secondary field and system geometry are treated as interdependent quantities and the GA-LEI inversion algorithm allows all three of these quantities to be varied to achieve a mutually consistent solution.

The inversion control file is contained in Appendix 2. The inversion output ASCII header information from the inversion is in Appendix 3.

2.2 Conductivity Reference Model

The starting point of the inversion is a conductivity reference model, which is iteratively adjusted until the data are fitted. The reference model is based on *a priori* borehole conductivity logs. Conductivity logs can be used, in principle, to create a detailed reference model that varies across the survey in order to constrain the inversion when the solution becomes ambiguous. In the Paterson survey, 19 conductivity logs were recorded and provide a first-pass approximation of conductivity for a regional-scale survey such as this.

Due to the number of conductivity logs, the reference model used in this inversion is simply a half-space of homogeneous conductivity across the survey. This reference model uses a conductivity value of 0.004 S/m, based on the average value of the resistive basement obtained from the logs. The limitations of this reference model assumption are discussed in the next chapter.

3 GA-LEI inversion products

3.1 Depth of Investigation

The inversion model is determined not only on the measured conductivity data, but also depends on an *a priori* estimate of conductivity. This estimate of conductivity, known as the reference model, is used as the starting point of the inversion and the solution is reached from iterative perturbations to the reference model. Since the reference model is simply a uniform half-space of conductivity (and thus an unrealistic model), it is important to ascertain how much the solution is determined by the reference model and how much it is determined by the AEM data itself.

The relative contributions of the data and the reference model can be estimated by defining a parameter called the percent data influence (PDI); which compares two inversions created from different reference models. In this work, the PDI is defined as:

$$PDI = 100\left(1 - \frac{\log(\sigma_{i1}) - \log(\sigma_{i2})}{\log(\sigma_{r1}) - \log(\sigma_{r2})}\right)$$

where σ_{i1} and σ_{i2} are the two inverted conductivities at a given location and σ_{r1} and σ_{r2} are the corresponding reference model conductivities (Lane *et al.*, 2004a). We define the PDI using the logarithm of the conductivity, since this is the quantity used in each inversion.

If the PDI is greater than 50% then the inversion is deemed to be more influenced by the AEM data than the reference model, whereas if it is less than 50% then the reference model is deemed to be dominant. The depth of investigation (DOI) is defined as the depth at which the PDI is 50%. Thus the DOI marks the depth to which the inverted conductivity is relatively robust. Note that the 50% PDI threshold is arbitrary and a different threshold could be chosen. **Figure 3** illustrates the effect of the DOI, showing an inverted section of line number 10040 data with two inverted solutions. In **Figure 3**a the inversion uses a reference conductivity of 0.04 S/m, whereas in **Figure 3**b the inversion uses a reference conductivity of 0.004 S/m.

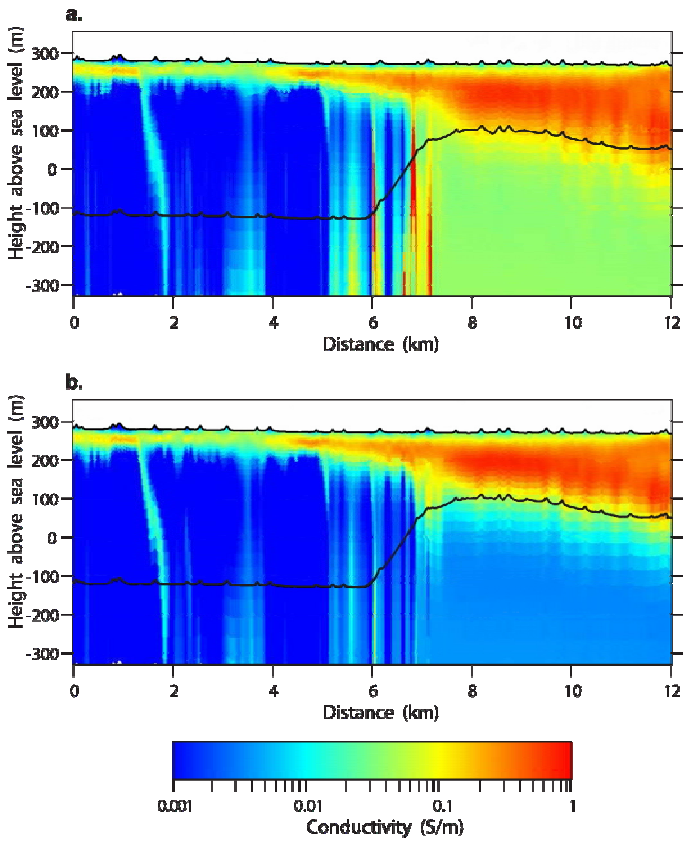

Figure 3: *Sample conductivity depth sections comparing the results of inversions using reference models of (a) 0.04 S/m and (b) 0.004 S/m. The black line marks the depth of investigation (DOI) in each case. Above the DOI, the results are similar for both inversions, whereas below the DOI the conductivity differs according to the reference model value.*

As shown in **Figure 3**, in the resistive areas of the inversion (predominantly blue), the solution is nearly identical under both reference models. This is reflected by the DOI threshold line being deeper in these areas. In more conductive areas, notably on the right hand side of the section, the deeper parts of the inversion are dominated by the reference model. Below the DOI the conductivity steadily approaches a homogeneous reference model value.

3.2 Grids

The Phase-2 data release contains a selection of 2D grids, presenting the inverted data across the whole Paterson survey. These 2D grids have been created in three different categories:
1. as single inversion layers (using the 30 layer GA-LEI model);
2. as depth slices; and
3. as elevation slices.
The depth slices are referenced using the distance to the surface at each point (thus its vertical shape is determined by the surface topography), whereas the elevation slices are referenced to the height above sea level.

All of these grids present the data using the (base-10) logarithm of conductivity, since this is the value that enters into the inversion. We have found that geological structures are more evident in grids that use the logarithm of conductivity, than conductivity itself. Users who wish to grid the data without logarithms may obtain the data from the raw inversion output file: *master.inversion.dat* (see Appendix 1).

3.2.1 Gridding parameters

The AEM survey data were gridded using Intrepid Software and are stored in binary files as ER Mapper single band IEEE4Byte Real data types. A comprehensive ER Mapper header (.ers) file is associated with each grid file, which describes the data type and the coordinate systems used to geographically position the grid. Gridded data are stored in a projected coordinate system only, in this case Universal Transverse Mercator (metric) coordinates of the Map Grid of Australia Zone 51 using the Geodetic Datum of Australia 1994. Technical details of the projection used are given in Appendix 4.

In the north-east corner of the survey the line spacing is 6 km. It was deemed more appropriate to not interpolate data across 6 km to reduce artefacts that obscure the structure evident in the data. In this area the data appears as coloured stripes with null values in between. This "Venetian blind" effect can be seen in the DOI grid, the depth slices and elevation slices (**Figure 4** to **Figure 6**).

3.2.2 AEM Go Map

The DOI (described in Section 4.1) is presented as a 2D grid in **Figure 4**. The probability of detection assumption required to cap the percent data influence (PDI) threshold, as discussed in Chapter 4, was set to 400 m, based on forward modelling in resistive terrain. In the resistive areas of the survey the DOI reaches this maximum depth. The yellow and red colours (40 - 150 m) in **Figure 4** are areas where the DOI is much shallower, and in some places is less than 100 m. These shallower areas of the DOI correspond closely to conductive regions of the survey area.

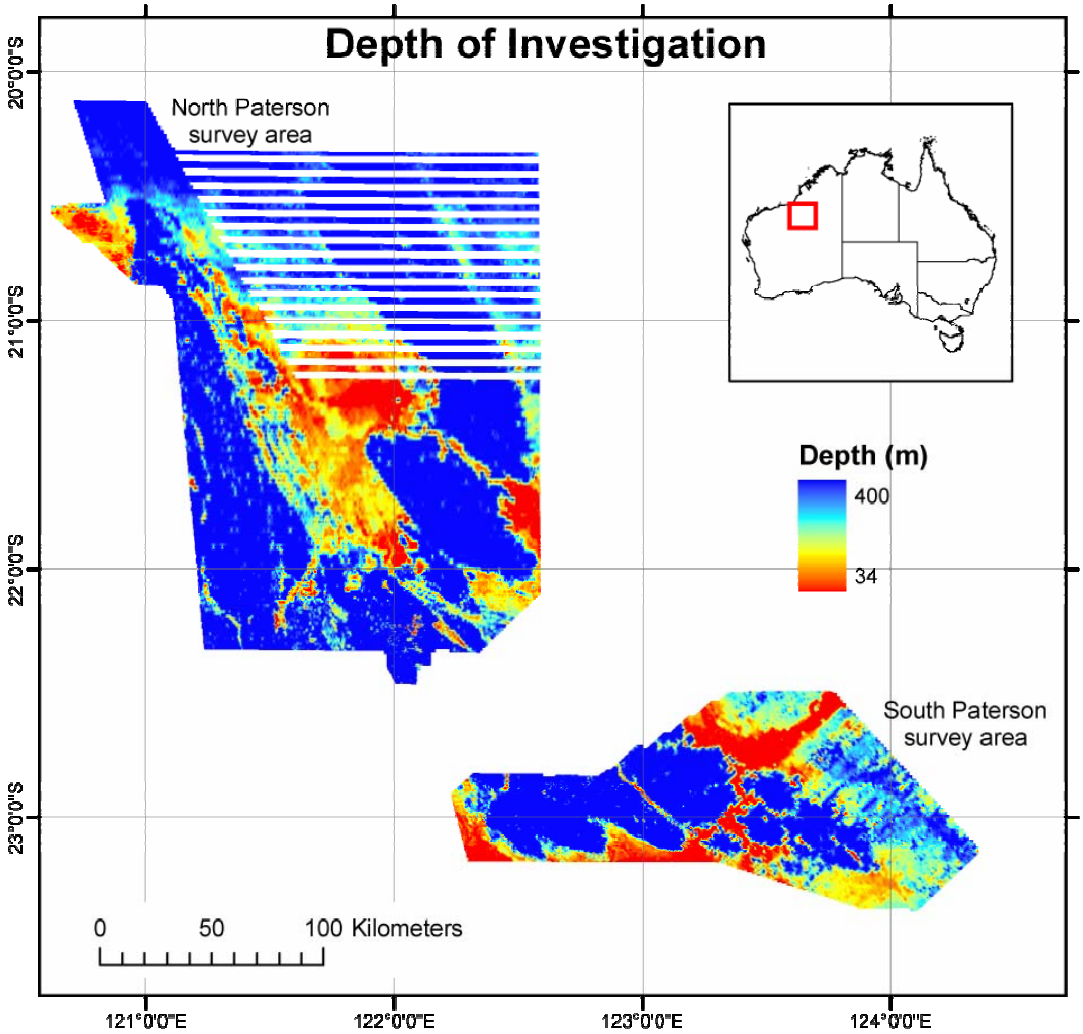

Figure 4: *The DOI grid.*

The DOI grid can also be used an "AEM Go Map", since it indicates where an AEM survey is able to penetrate to substantial depths. In areas where the DOI is deep, an AEM survey will be a useful tool to investigate the geology at depth. In contrast, if the DOI is shallow, an AEM survey will only provide useful information near the surface.

The main grid products of this AEM inversion are the depth slices and elevation slices. These grids present the inverted conductivity values in 2D spanning the entire survey area. The DOI surface has been incorporated into these depth and elevation slice grids in order to mask out results that are predominantly driven by the choice of reference model. The purpose of this masking is to focus attention on the data-driven results of the inversion and to ensure that spurious features from model-driven results are not misinterpreted as real structures or objects.

3.2.3 Depth Slices

A series of 13 depth slices have been created between 0 and 300 m, with the slices becoming progressively thicker with depth. The depth slices are set to 5 m thickness between 0 and 20 m depth, 10 m thickness between 20 and 40 m depth, 20 m thickness between 40 and 100 m depth, and

50 m thickness between 100 and 300 m depth. These increases in thickness reflect the higher sensitivity of the inversion at shallower depths.

A selection of four depth slices is illustrated in **Figure 5**, showing (6a) 0-5 m, (6b) 30-40 m, (6c) 100-150 m, and (6d) 200-250 m. Both **Figure 5**a and **Figure 5**b show a range of conductive and resistive areas and there is no DOI masking, since the depth slices are relatively shallow. However, **Figure 5**c shows some isolated areas of DOI masking, and **Figure 5**d shows substantial masking in broad conductive regions. This masking reflects the different penetration of the AEM signal in resistive (deep penetration) and conductive (shallow penetration) areas.

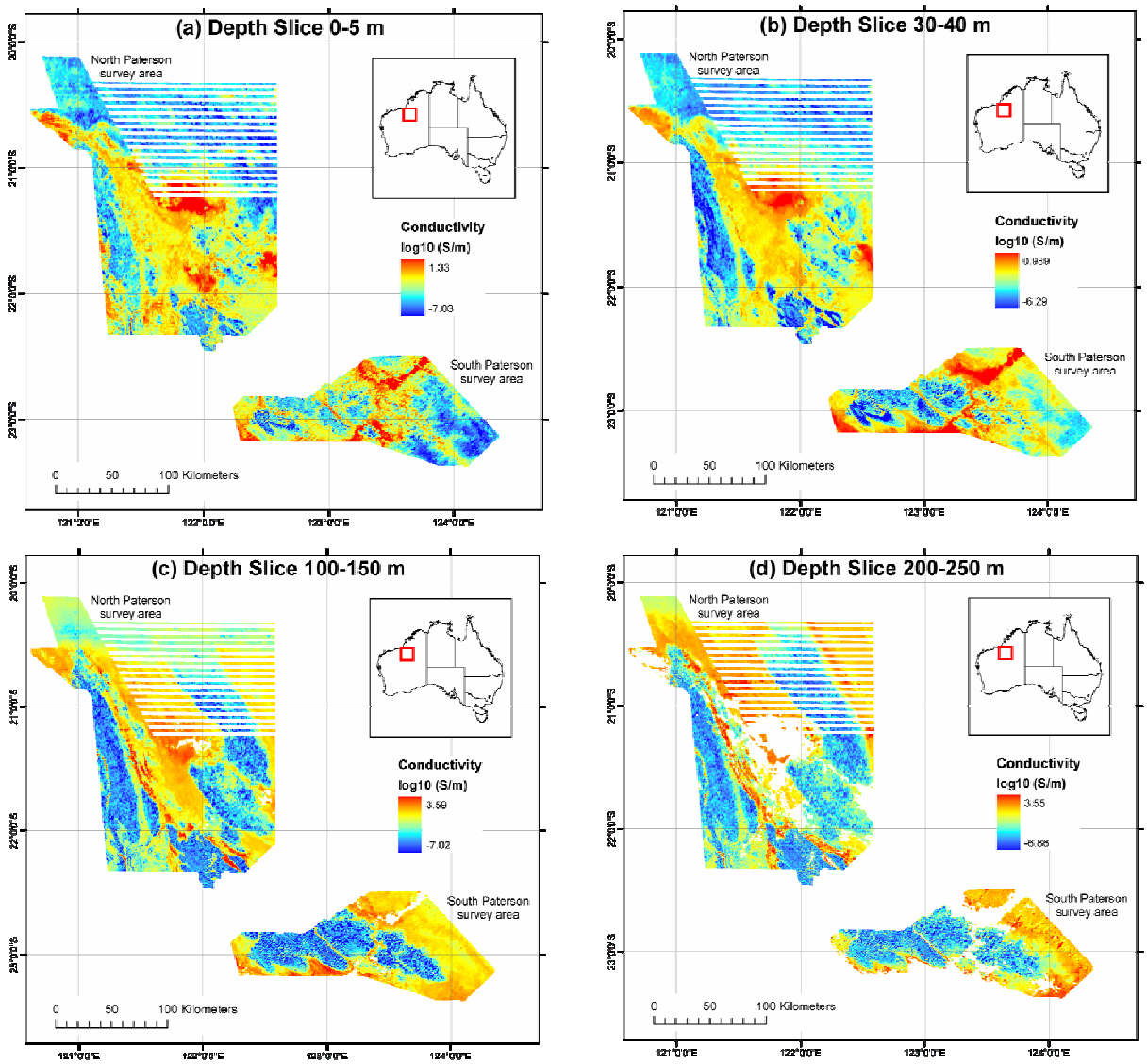

Figure 5: *A selection of depth slices showing a) 0-5 m, b) 30-40 m, c) 100-150 m and d) 200-250 m. Data falling below the DOI have been masked out, and appear white.*

3.2.4 Elevation slices

The elevation slices present the same inversion results, but the slices are referenced to the height above sea level rather than depth below surface. This gives the option of viewing data plotted along

horizontal planes. The one drawback of using elevation slices over the entire survey is that there is a substantial altitude difference across some parts of the Paterson survey - up to 400 m of relief between the highest and lowest points of the survey. Therefore a given elevation slice may compare near-surface data from one corner of the survey with much deeper data from other parts of the survey.

Elevation slices were created from 490 m below sea level to 540 m above sea level at 10 m intervals. **Figure 6**a-d shows a selection of the elevation slices, with (**Figure 6**a) 0-10 m, (**Figure 6**b) 100-110 m, (**Figure 6**c) 200-210 m and (**Figure 6**d) 300-310 m above sea level. In both **Figure 6**a and **Figure 6**b there are substantial areas of masking due to the DOI, as parts of these slices lie deep below the surface. In **Figure 6**c and **Figure 6**d there is little or no masking from the DOI, but there are still substantial areas of null data values due to the land surface being lower than the elevation slice itself. These null data values are especially prevalent in the north-west, where the surface elevation is significantly lower, and hence much of this area is below the 300 m altitude of the elevation slice.

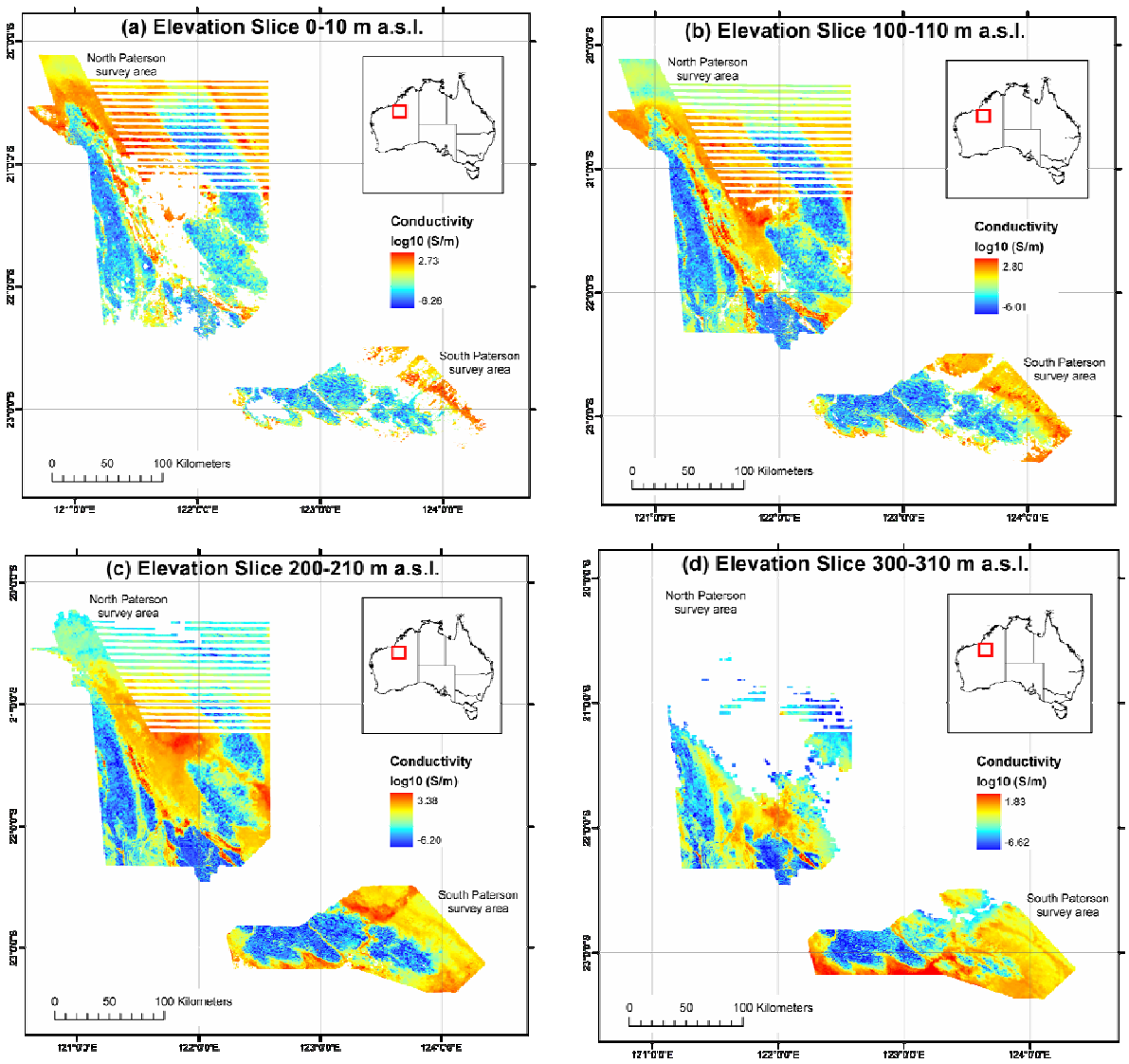

Figure 6: *Selection of elevation slices, showing a) 0-10 m above sea level (a.s.l.), (b) 100-110 m a.s.l., (c) 200-210 m a.s.l. and (d) 300-310 m a.s.l.*

3.3 Sections

Vertical sections of GA-LEI's and multiplots are provided as a quick reference tool as both georeferenced jpegs and non georeferenced multiplots. The PDI is marked in black on the GA-LEI's and is contained within the associated databases.

3.3.1 Georeferenced jpegs

The JPEG World file is used to georeference JPEG (.jpg) files. The .jgw files provide coordinate information to the associated file. Each of the Paterson flight lines has a GA-LEI image stored as a jpeg (jpg) file and an associated (.jgw) file (**Table 3**).

Table 3: JPEG world file contents for line 10000

COLUMN	DATA
1 x scale (per pixel)	4.225161
2 rotation about y axis	0.020241
3 rotation about x axis	0.020241
4 y scale	-4.225161
5 x reference point	397076.753108
6 y reference point	7541178.552010

Georeferenced jpegs have been included in the Phase-2 data release as a convenient way to overlie inversion data into GIS software (**Figure 7**). There is no other data contained within the plot and the colour bar is found in the georeferenced jpeg data file directory and applies to all sections (**Figure 8**).

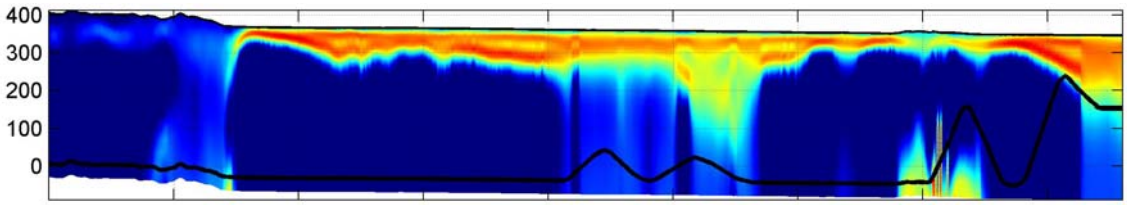

Figure 7*: Georeferenced jpeg for line 10000. Elevation above sea level is in metres and is labelled on the left hand side of each plot. The horizontal scale is provided in the accompanying .jgw world file.*

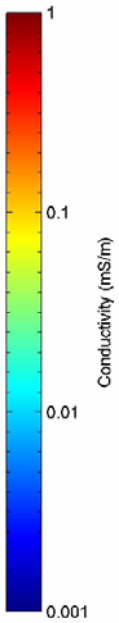

Figure 8*: Colour bar for georeferenced jpegs. One colour bar is provided to reference to all lines.*

3.3.2 GA-LEI multiplots

The GA-LEI multiplots (example shown in **Figure 9**) for the Paterson AEM survey contains a number of panels which include:

Phi_D	- the data misfit of the inversion, the target misfit is less than 1.0
TX Height	- Transmitter height in metres
TX att	- Transmitter attitude in degrees with two traces measuring the pitch and roll
D_x	- Inline horizontal separation between the transmitter and the receiver coils in metres. Two traces measuring the processing estimate and inversion output
D_z	- Inline vertical separation between the transmitter and the receiver coils (D_z) in metres. Two traces measuring processing estimate and inversion output
R_p	- Receiver pitch in degrees. Two traces measuring the processing assumption and inversion output
asinh (X)	- Window amplitude profiles for X component data (fT) compressed using the asinh function to give an overview of the decay along line for non-geometry corrected data
asinh (Z)	- Window amplitude profiles for Z component data (fT).
GA-LEI	- image in depth below surface (m) with conductivity colour bar in (S/m).
Easting	- labelled every 5000m
Northing	- labelled every 5000m

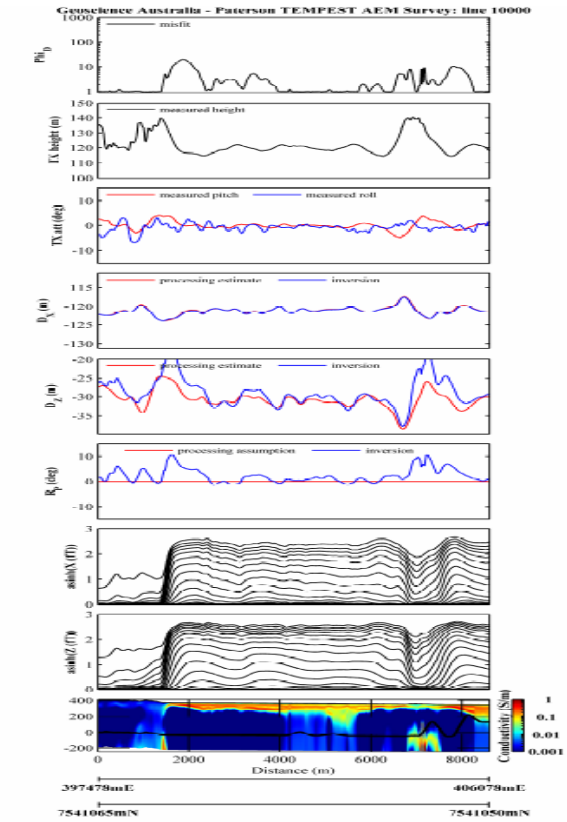

Figure 9*: GA-LEI multiplot for line 10000.*

3.4 Discrete conductors

The primary reason for conducting the AEM survey in the Paterson area is to map regional geology, as well as potential unconformity-, palaeochannel- and calcrete-related uranium deposit host rocks. However, as a procedural step in the QA/QC process, the data were scanned for the presence of discrete conductors.

Multiplots delivered by FAS were used for interpreting the presence of discrete conductors using the process described in Lane and Worrall (2002). The transmitter loop and receiver coil variations are observed in windowed amplitude responses when system geometry, receiver coil vibration and "sferics" exist. Sferics are noise caused by lightning flashes within about 1500 km of the survey area. It is important to determine if the source of the discrete conductor effect is noise or variations in the subsurface conductivity distribution. **Figure 10** shows an example of an X and Z component multiplot for line 20641, with a discrete conductor feature at fiducial 1410.

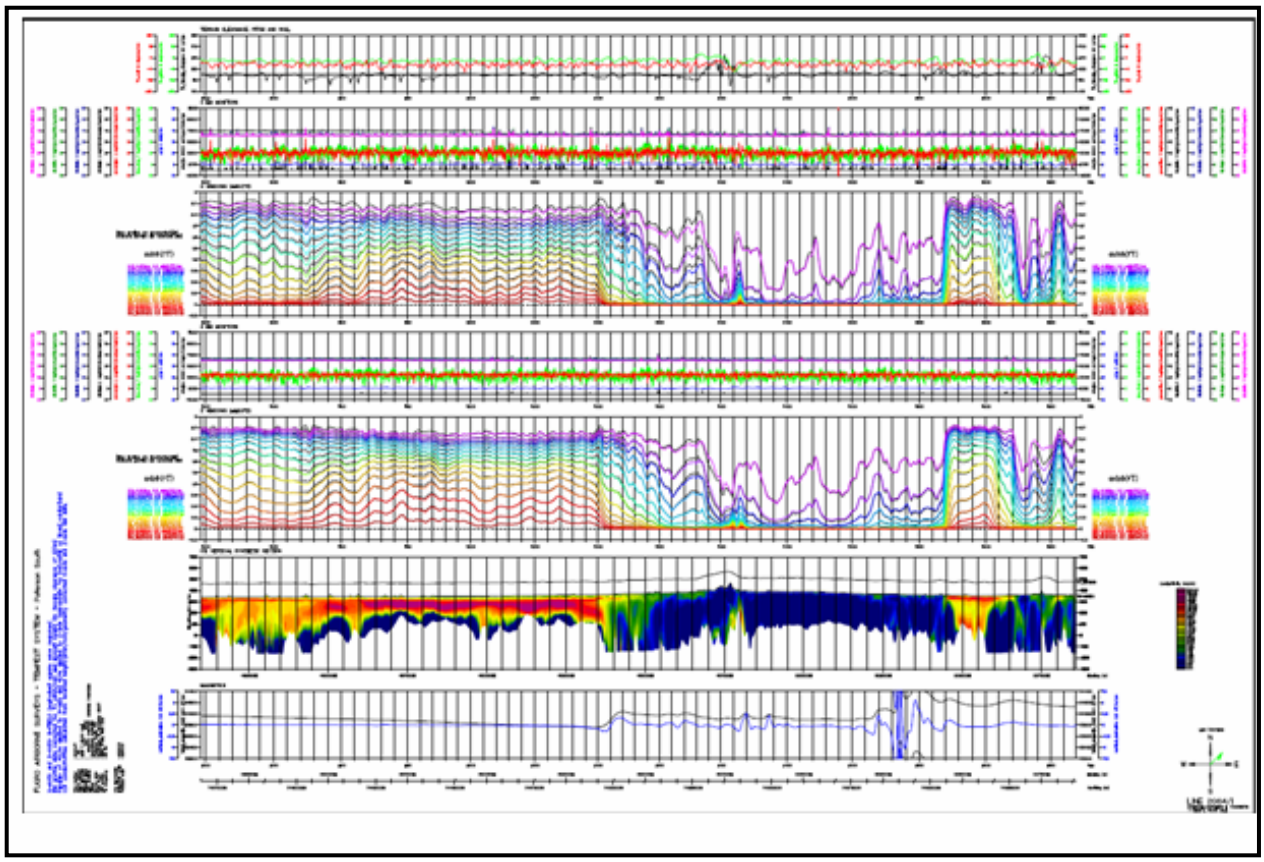

Figure 10*: A FAS multiplot for line 20641 from the Paterson South survey area.*

Multiplot 20641 is expanded in **Figure 11** to highlight the discrete anomaly that is present at fiducial 1410.

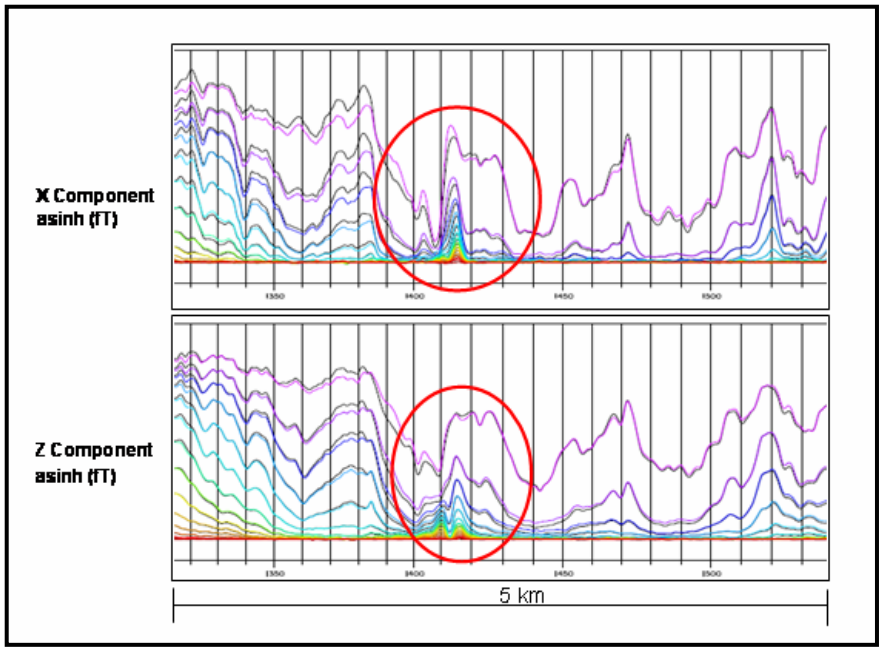

Figure 11: *Sub-section of the multiplot for line 20641 highlighting the discrete conductor response in the X and Z component windows.*

Figure 12 shows a comparison subsection of EMFlow to the GA-LEI conductivity section for line 20641.

a)

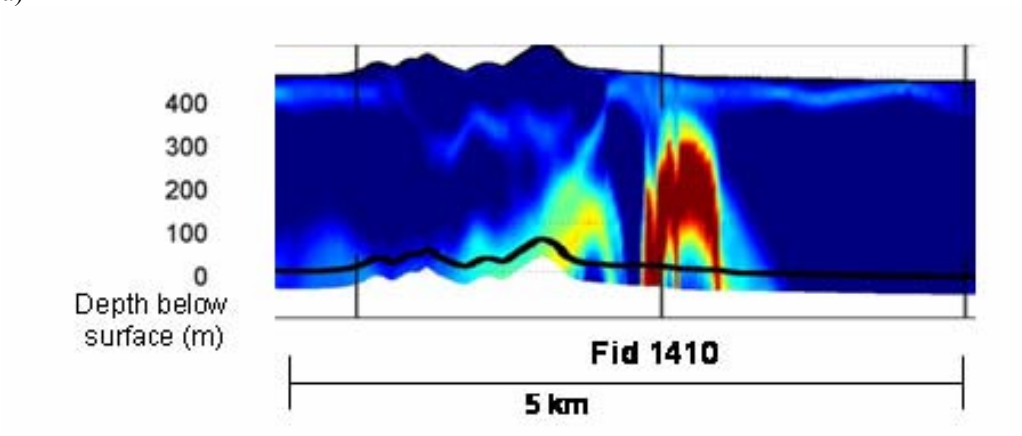

b)

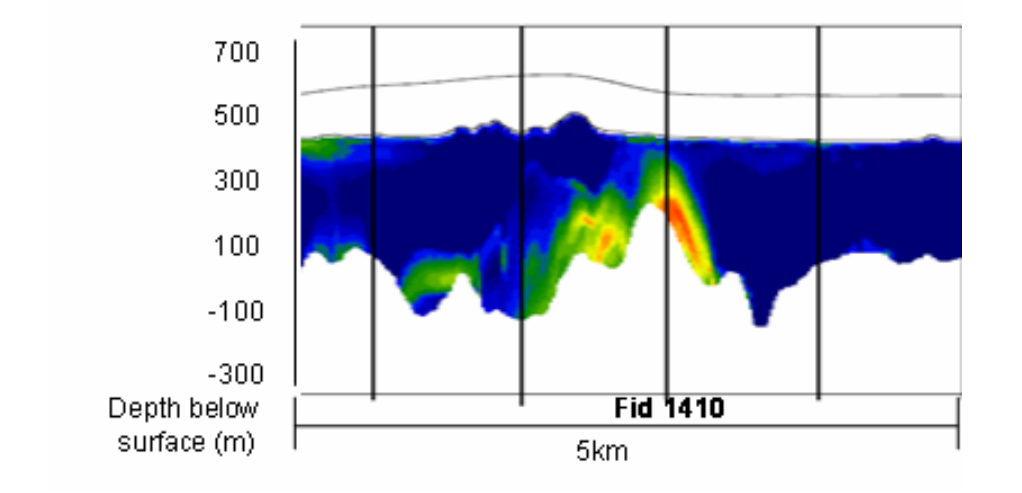

Figure 12*: A comparison between EMFlow and GA-LEI conductivity sections for line 20641. a). Subsection of the GA-LEI inversion for line 20641 highlighting the discrete conductor response. b). Subsection of the FAS EMFlow CDI for line 20641. Please note the vertical exaggeration differs between plots.*

4 Validation

4.1.1 Conductivity Logging

A conductivity logging program was conducted in the Paterson survey area to help validate the survey data. Geoscience Australia would like to acknowledge Aditya Birla Minerals – Birla Nifty Operations, Consolidated Minerals – Woodie Woodie Operations and Newcrest Mining Limited – Telfer Operations for land access, access to open bore holes, lithological logs and field support. Some of the company data remain "in-confidence" and are not expanded upon further in this report.

Induction conductivity data was acquired in boreholes (referred to as conductivity logs) during September 2009 in support of the Paterson AEM survey. The data were acquired from a number of widespread boreholes across different geological formations. The logs are used to assist in generating reference models for geophysical inversions of the AEM data, as well as allowing the results of those inversions to be assessed against an independent dataset (Sorensen, 2008).

Nineteen boreholes distributed across the Paterson North area were logged with an induction conductivity logging tool. No boreholes in the Paterson South area were logged due to the fact that there were no open holes available at the time of the fieldwork. Three boreholes were located at Telfer mine (Newcrest), five were at Woodie Woodie (Consolidated Minerals) and two were waterbores located on Telfer Access Road. The remaining bores were either waterbores or exploration bores at and around Nifty mine (Aditya Birla). Most of the holes were cased with PVC, but a few were open, un-cased holes. The majority of the holes had steel casing in the top 6 m (Sorensen, 2008).

Table 4 provides location coordinates and depths of the logged boreholes and **Figure 13** shows the location of the logged boreholes plotted over the conductance from 0-200 m. The five conductivity logs collected at Woodie Woodie are "in-confidence", and are not displayed.

Induction conductivity logging tools measure the electrical conductivity of the material surrounding the borehole and provide a detailed indication of changes in conductivity with depth. These tools permit measurements of the electrical conductivity of the ground outside PVC cased boreholes - generally without being sensitive to the presence of more conductive borehole fluid within the casing. These tools are capable of making reliable scientific measurements, however, their method of use has not been standardised. The principle of operation of inductive conductivity borehole logging tools (McNeill, 1986) and other conductivity logging information can be found in Appendix 5 (see also Sorensen and Lane, 2007b).

In order to validate the predictions of the inversion, we compare the results of the GA-LEI at selected points to the borehole conductivity logs collected in the survey area. Since there are only 19 borehole logs compared to 29 000 line km of AEM data, this validation applies to only a small sample of the inversion.

The results of these comparisons for the 14 publicly available conductivity logs are shown in **Figure 14** to **Figure 17**. Each borehole log is compared to the nearest point of the inversion. On each plot, "PhiD" measures the data misfit of the inversion (the target misfit is less than 1.0), and "distance" represents the distance from the nearest point of the inversion to the borehole location. The distances vary from 137 m to 769 m, and the average distance is 441 m. These distances are generally larger than the footprint of the AEM signal, thought to be approximately 300 m, so the comparisons should be thought of as indicative, rather than a precise ground-truth measurement of the results.

Table 4: Coordinates (MGA94 Zone 51) and depths of the 19 boreholes

BOREHOLE	EASTING	NORTHING	DEPTH (m)
08DKRCD011	348403	7657601	428
08DKRCD012	348074	7657600	561
08FCHDD002	361302	7590049	285
THRP155	356024	7600376	119
THRP161B	358531	7600035	159
THRP162D	351524	7603738	60
Waterbore B	351524	7604678	125
YNC219	352665	7603678	200
YNC224	352750	7603643	100
WW1	In confidence	In confidence	101
WW2	In confidence	In confidence	120
WW3	In confidence	In confidence	39
WW4	In confidence	In confidence	120
WW5	In confidence	In confidence	62
HB405	373788	7624508	46
HB419	307618	7643890	34
HB326	423671	7589789	148
HB315	420467	7590932	150
HB227	416363	7602972	156

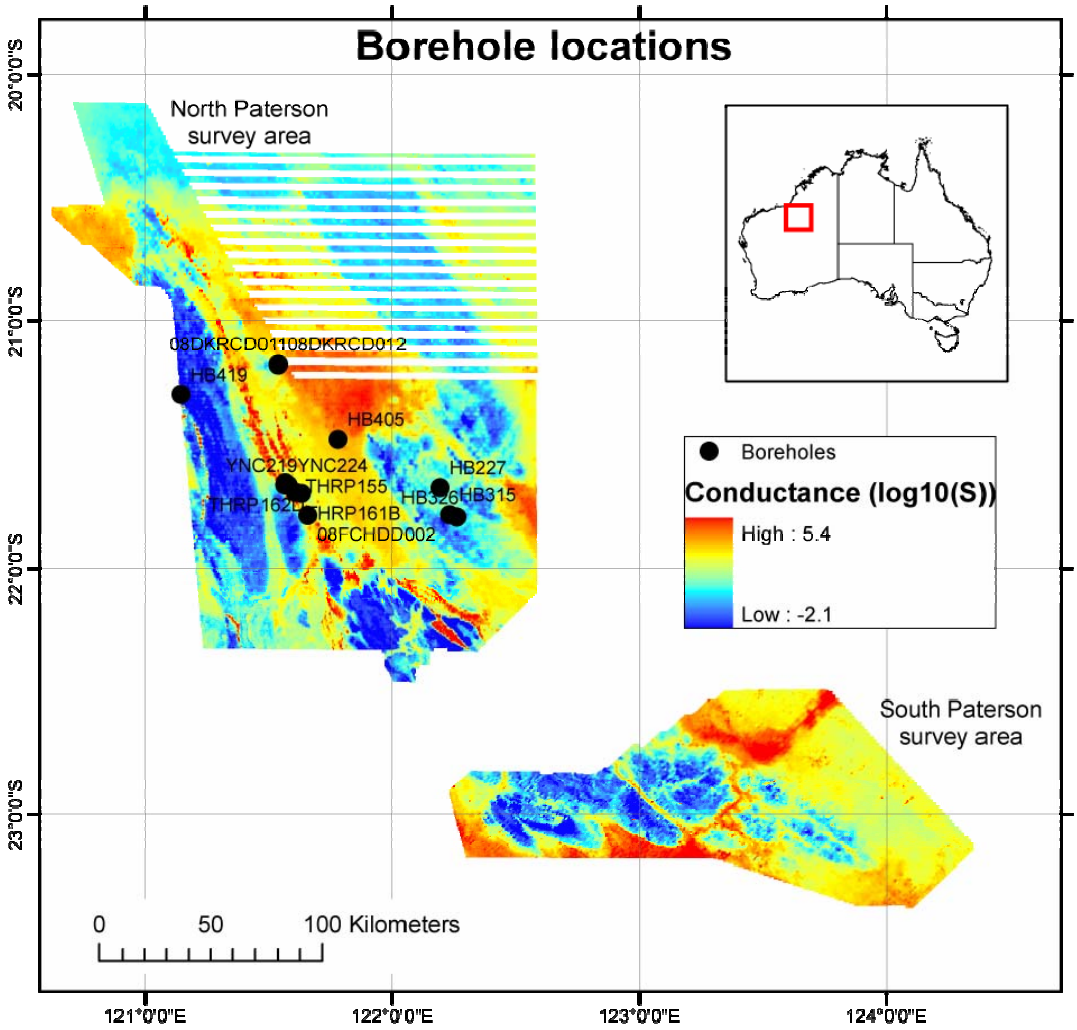

Figure 13*: The location of the boreholes plotted over conductance from 0-200 m..*

Generally, the GA-LEI results show agreement with of the borehole logs in close proximity to flight lines. The GA-LEI results are smoother than the borehole logs, due to the vertical smoothness constraints of the GA-LEI. Although some localised features of the borehole logs are missing in the GA-LEI, the major conductivity trends are well represented by the inversion.

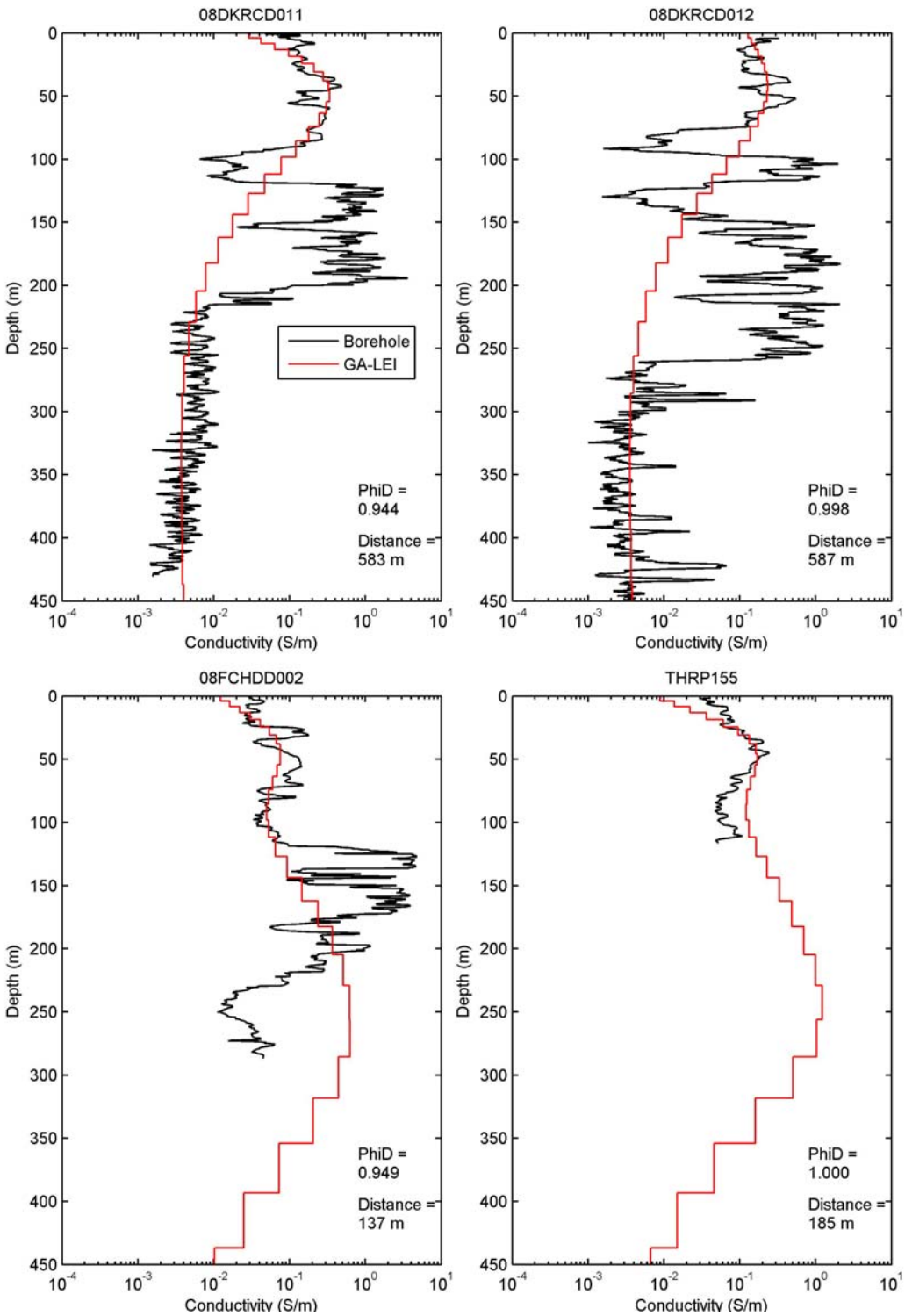

Figure 14: *Conductivity logs compared to GA-LEI results.*

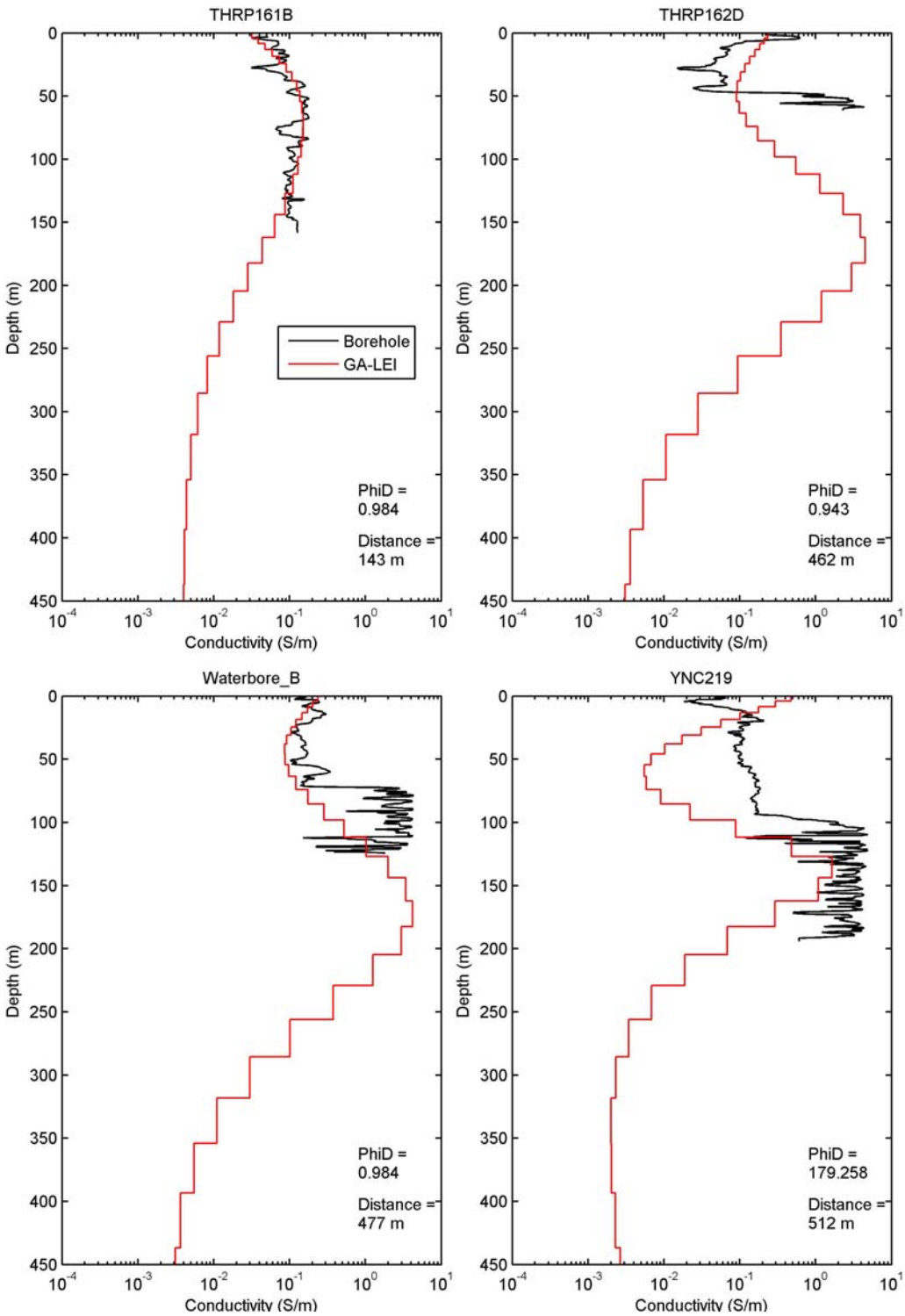

Figure 15: *Conductivity logs compared to GA-LEI results (continued).*

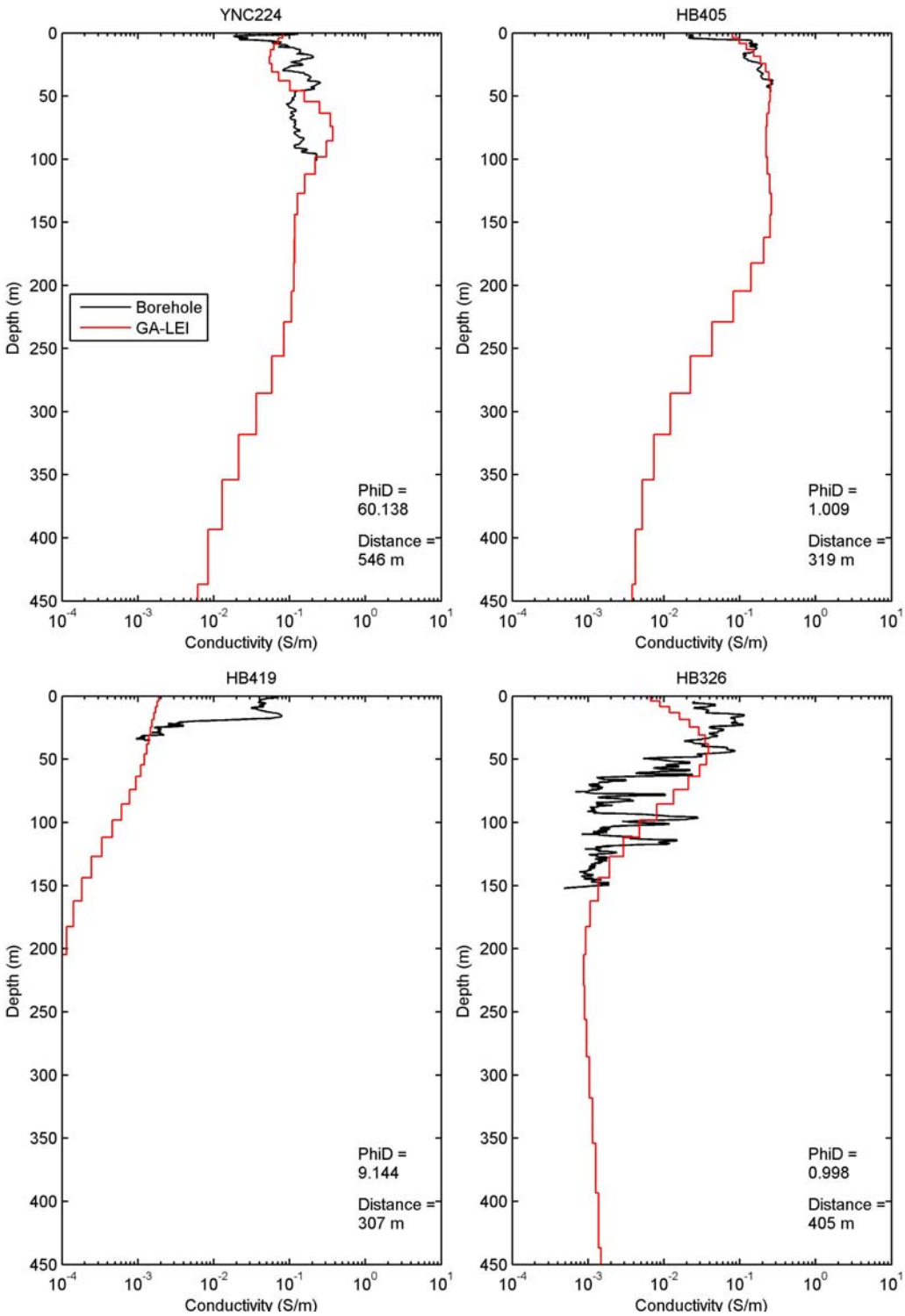

Figure 16: *Conductivity logs compared to GA-LEI results (continued).*

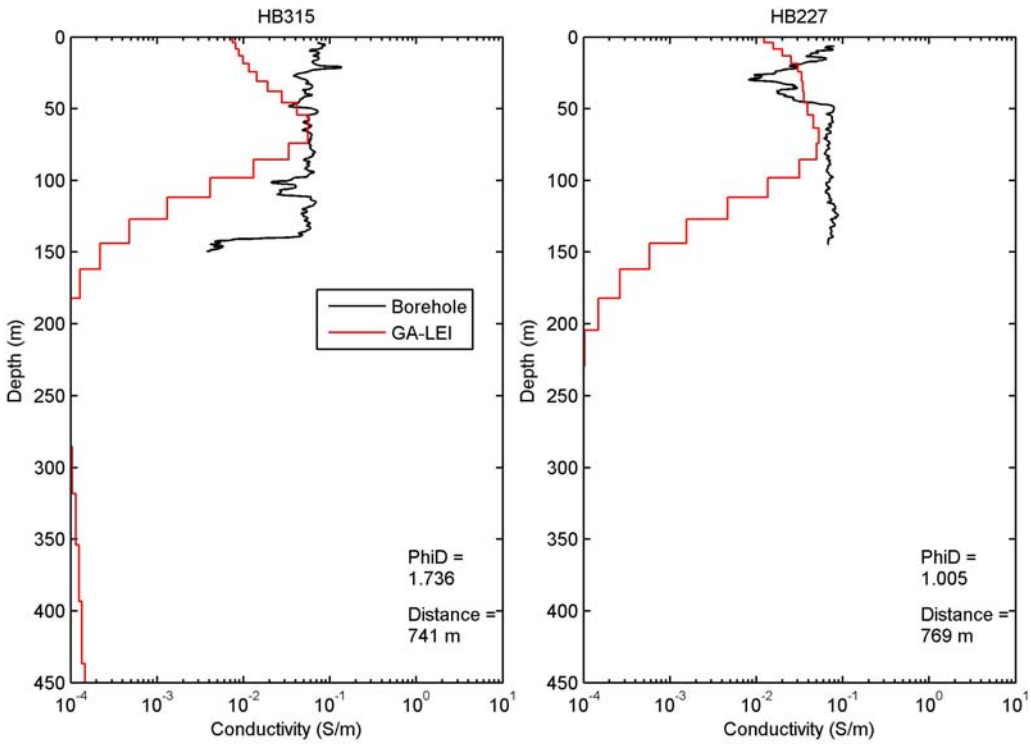

Figure 17: *Conductivity logs compared to GA-LEI results (continued).*

5 Summary

The Phase-2 data release presents conductivity predictions, at depths of several hundred metres across the Paterson region. The data reveal major subsurface structures of geological and hydrogeological units, including graphitic units in the Rudall Complex, Permian paleovalleys and other regolith features. The inversions use a 30-layer sample-by-sample inversion using the GA-LEI algorithm, which solves for both conductivity data and the AEM system geometry. This algorithm represents a significant improvement on the Phase-1 data, in mapping conductivity in greater detail and identifying features such as unconformities and major structures.

The conductivity predictions are presented as both line sections and grid formats. Line sections are produced as georeferenced JPEG files of conductivity at depth, and as multiplots that display conductivity with AEM system geometry measurements along each line. Grid products include conductivity depth and elevation slices, conductance, and the AEM Go Map. These products can enhance our understanding of the geology in the Paterson region, and can be used to guide further exploration by industry.

6 Acknowledgements

Geoscience Australia would like to acknowledge the contributions of the following groups: Aditya Birla Minerals – Birla Nifty Operations for field support as well as land access, access to open bore holes, lithological logs; Consolidated Minerals – Woodie Woodie Operations and Newcrest Mining Limited – Telfer Operations for access to open bore holes and lithological logs; subscription companies Rio Tinto, Cauldron Energy, Cameco, Mega Uranium and Western Areas, for their support of the AEM project by funding additional lines, supplying historical data and providing geological support; the Western Desert Land Aboriginal Corporation (WDLAC) for granting access the traditional lands of the Martu people; Geological Survey of Western Australia; Geophysics Group at Geoscience Australia.

7 References

Brodie, R and Fisher, A., 2008. Inversion of TEMPEST AEM survey data, Honeysuckle Creek, Victoria. Unpublished report produced by Geoscience Australia for the Bureau of Rural Sciences.

Constable, S., Parker, R., and Constable, C., 1987. Occam's inversion; a practical algorithm for generating smooth models from electromagnetic sounding data. *Geophysics*, **52,** 289-300.

Costelloe, M., Whitaker, A., Brodie, R., Fisher, A. and Sorensen, C., 2007. Paterson airborne electromagnetic survey, Onshore Energy and Minerals, Geoscience Australia. *ASEG Extended Abstracts 2007*.

Lane, R., Green, A., Golding, C., Owers, M., Pik, P., Plunkett, C., Sattel, D., Thorn, B., 2000. An example of 3D conductivity mapping using the TEMPEST airborne electromagnetic system. *Exploration Geophysics*, **31**, 162-172.

Lane, R. and Worrall, L., 2002. Interpretation of Airborne Electromagnetic Data: Summary report on the Challenger Workshop. Gawler Craton Mineral Promotion Project Record. 2002/2.

Lane, R., Brodie, R. and Fitzpatrick, A., 2004a. Constrained inversion of AEM data from the Lower Balonne area, Southern Queensland, Australia. CRC LEME Open File Report 163.

Lane, R., Brodie, R., and Fitzpatrick A., 2004b. A revised inversion model parameter formulation for fixed wing transmitter loop – towed bird receiver coil time-domain airborne electromagnetic data. ASEG 17th Geophysical Conference and Exhibition, Sydney 2004.

Lawrence, M. and Stenning, L., 2007a. Paterson North Airborne Electromagnetic (AEM) Mapping Survey Acquisition and Processing Report for Geoscience Australia

Lawrence, M. and Stenning, L., 2007b. Paterson South Airborne Electromagnetic (AEM) Mapping Survey Acquisition and Processing Report for Geoscience Australia

Macnae, J., King, A., Stolz, N., Osmakoff, A., Blaha, A.,1998. Fast AEM processing and inversion: *Exploration Geophysics* **29**, 163-169.

McNeill, J.D., 1986. Geonics EM39 borehole conductivity meter-theory of operation: Mississauga. *Ontario, Geonics Ltd., Technical Note* **20(11)**.

Reid, J.E., and Brodie, R.C., 2006. Preliminary inversions of Honeysuckle Creek airborne electromagnetic data: Comparison with borehole conductivity logs and

previously derived conductivity models. Unpublished report produced by Geoscience Australia for the Bureau of Rural Sciences.

Roach, I.C., (editor), 2010. Geological and energy implications of the Paterson Province airborne electromagnetic (AEM) survey. *GA Record* **2010/12**. (*July 2010*).

Sorensen, C. and Lane, R., 2007a. Billabong Creek: Notes on reprocessing of the AEM data using GA-LEI. Unpublished report produced by Geoscience Australia for the Bureau of Rural Sciences.

Sorensen, C. and Lane, R., 2007b. Guidelines for conductivity borehole logging procedures. Unpublished GA internal report.

Sorensen, C., 2007. Assessment of AEM systems for the Paterson survey. Unpublished GA internal report (in-confidence).

Sorensen, C., 2008. Logistics report for down-hole conductivity logging in the Paterson AEM Survey area, Western Australia, September 2008. Unpublished GA internal report.

Stolz, E., and Macnae, J., 1998. Evaluating EM waveforms by singular-value decomposition of exponential basis functions: *Geophysics*, **63**, 64-74.

Smith, R.S., 2001a. On removing the primary field from fixed wing time-domain airborne electromagnetic data: some consequences for quantitative modelling, estimating bird position and detecting perfect conductors. *Geophysical Prospecting*, 49, 405-416.

Appendix 1 Accompanying DVD

NAME	FORMAT	DESCRIPTION	COMMENTS
linedata			
master.inversion.dat master.inversion.hdr	Ascii hdr	ascii data file containing master inversion output (reference model = 0.004 S/m) associated header information in text format	1 file containing 681 lines of data 1 txt file containing 125 lines of data
secondary.inversion.dat secondary.inversion.hdr	Ascii hdr	ascii data file containing inversion output used to calculate pdi (reference model = 0.04 S/m) associated header information in text format	1 file containing 681 lines of data 1 txt file containing 125 lines of data
eintervals_10m.dat eintervals_10m.hdr	Ascii hdr	ascii data file containing inversion output sliced into 10 m elevation intervals associated header information in text format	1 file containing 681 lines of data 1 txt file containing 82 lines of data
sections			
GA_LEI_georeferenced_jpeg	.jpeg and associated .jgw	georeferenced line sections of conductivity	Linenumber.jpg Linenumber.jgw
GA_LEI_multiplots	.pdf	line sections of conductivity, compared with AEM system geometry and data misfit.	Linenumber.pdf
grids			
Depth Slices	.ers	conductivity grids in slices of depth below surface	15 .ers files
Elevation slices	.ers	conductivity grids in slices of elevation above sea level (10 m and 50 m slices)	90 .ers files
Conductance	.ers	total conductance grids for 0-200m and 0-400m depth	2 .ers files
AEM Go Map	.ers	depth of investigation grid	1 .ers file
conductance_jpeg	.jpeg and associated .jgw	georeferenced grids conductance	2 .ers files
depth_slice_jpeg	.jpeg and associated .jgw	georeferenced grids depth slices	15 .ers files
elevation_slice_jpeg	.jpeg and associated .jgw	georeferenced grids elevation slices	90 .ers files
AEM_Go_Map_jpeg	.jpeg and associated .jgw	georeferenced grid AEM Go Map	1 .ers file

report			
Paterson_Phase-2_report.pdf	.pdf	Explanatory notes	1 file
shapefiles			
Flight Lines Survey Boundary National Park	.shp	Three Paterson survey shape files and associated files	19 files

Appendix 2 Inversion control file

```
Control Begin

        LogFile  = inversion.output.log
        InfoFile = inversion_info.txt

        Matlab Begin
                Call = no
                PostIterationMFile = E:\matlab\post_iteration.m
                PostSampleMFile    = E:\matlab\post_sample.m
                DumpPath = results\
        Matlab End

        EMSystem Begin
                SystemFile = Tempest-075k.stm
                NumberOfWindows = 15
                UseXComponent   = yes
                UseYComponent   = no
                UseZComponent   = yes

                InvertTotalField = yes
                ReconstructPrimaryFieldFromInputGeometry = yes

                EstimateNoiseFromModel = yes
                XMultiplicativeNoise   = 2.9
                XAdditiveNoise = 0.0108          0.0079   0.0077   0.0057   0.0049   0.0049   0.0046
0.0044   0.0042   0.0042   0.0043   0.0038   0.0033   0.0023   0.0024
                ZMultiplicativeNoise   = 3.11
                ZAdditiveNoise  = 0.0072         0.0063   0.0056   0.0042   0.0041   0.0041   0.0038
0.0037   0.0035   0.0032   0.0032   0.0028   0.0023   0.0016   0.0021
        EMSystem End

        Earth Begin
                NumberOfLayers = 30
        Earth End

        Options Begin
                SolveConductivity = yes
                SolveThickness    = no

                SolveTX_Height = no
                SolveTX_Roll = no
                SolveTX_Pitch = no
                SolveTX_Yaw = no
                SolveTXRX_DX = yes
                SolveTXRX_DY = no
                SolveTXRX_DZ = yes
                SolveRX_Roll = no
                SolveRX_Pitch = yes
                SolveRX_Yaw = no
```

```
                LambdaChoiceMethod   = TargetLineSearchandStepFactor

                AlphaConductivity = 1.0
                AlphaThickness    = 0.0
                AlphaGeometry     = 1.0
                AlphaSmoothness   = 100000 //Set to 0 for no vertical conductivity smoothing

                WeightConductivityReferenceByLayerThickness = yes
                WeightSmoothnessByLayerThickness = yes

                MinimumPhiD = 1.0
                MinimumPercentageImprovement = 1.0
                MaximumIterations = 100
        Options End

        InputOutput Begin
                InputFile   =
\\nas\oemd\aem\aem\Paterson\aemdata\lines_survey_em\paterson_survey_lines_em.dat
                HeaderLines = 0
                Subsample   = 1

                OutputDataFile   = inversion.output.asc
                OutputHeaderFile = inversion.output.hdr

                Columns Begin
                        SurveyNumber    = Column 5
                        DateNumber      = Column 7
                        FlightNumber    = Column 2
                        LineNumber      = Column 1
                        FidNumber       = Column 3
                        Easting         = Column 12
                        Northing        = Column 13
                        GroundElevation = Column 17
                        Altimeter       = Column 14

                        TX_Height       = Column 21
                        TX_Roll         = Column 20
                        TX_Pitch        = -Column 19
                        TX_Yaw          = 0
                        TXRX_DX         = Column 22
                        TXRX_DY         = 0
                        TXRX_DZ         = Column 23
                        RX_Roll         = 0
                        RX_Pitch        = 0
                        RX_Yaw          = 0

                        ReferenceModel Begin
                                TXRX_DX      = Column 22
                                TXRX_DZ      = Column 23
                                RX_Pitch     = 0
                                Conductivity = 0.004
                                Thickness    = 4.00 4.40 4.84 5.32 5.86 6.44 7.09 7.79 8.57 9.43
10.37 11.41 12.55 13.81 15.19 16.71 18.38 20.22 22.24 24.46 26.91 29.60 32.56 35.82 39.40 43.34
47.67 52.44 57.68
```

```
                    ReferenceModel End

                    StartModel Begin
                        TXRX_DX      = Column 22
                        TXRX_DZ      = Column 23
                        RX_Pitch     = 0
                        Conductivity = 0.004
                        Thickness    = 4.00 4.40 4.84 5.32 5.86 6.44 7.09 7.79 8.57 9.43
10.37 11.41 12.55 13.81 15.19 16.71 18.38 20.22 22.24 24.46 26.91 29.60 32.56 35.82 39.40 43.34
47.67 52.44 57.68
                    StartModel End

                    StdDevReferenceModel Begin
                        TXRX_DX      = 1.0
                        TXRX_DZ      = 1.0
                        RX_Pitch     = 1.0
                        Conductivity = 3.0
                        Thickness    = 0.0
                    StdDevReferenceModel End

                    XComponentPrimary = UNAVAILABLE
                    YComponentPrimary = UNAVAILABLE
                    ZComponentPrimary = UNAVAILABLE

                    XComponentSecondary = Column 27
                    YComponentSecondary = UNAVAILABLE
                    ZComponentSecondary = -Column 65

                    StdDevXComponentWindows = UNAVAILABLE
                    StdDevYComponentWindows = UNAVAILABLE
                    StdDevZComponentWindows = UNAVAILABLE
                Columns End
            InputOutput End
Control End
```

Appendix 3 Conductivity data header information

This the conductivity data header information

1	uniqueid	48	conductivity:27	95	x_window_predicted:14
2	survey	49	conductivity:28	96	x_window_predicted:15
3	date	50	conductivity:29	97	z_primary_predicted
4	flight	51	conductivity:30	98	z_window_predicted:1
5	line	52	thickness:1	99	z_window_predicted:2
6	fid	53	thickness:2	100	z_window_predicted:3
7	easting	54	thickness:3	101	z_window_predicted:4
8	northing	55	thickness:4	102	z_window_predicted:5
9	elevation	56	thickness:5	103	z_window_predicted:6
10	altimeter	57	thickness:6	104	z_window_predicted:7
11	tx_height	58	thickness:7	105	z_window_predicted:8
12	tx_roll	59	thickness:8	106	z_window_predicted:9
13	tx_pitch	60	thickness:9	107	z_window_predicted:10
14	tx_yaw	61	thickness:10	108	z_window_predicted:11
15	txrx_dx	62	thickness:11	109	z_window_predicted:12
16	txrx_dy	63	thickness:12	110	z_window_predicted:13
17	txrx_dz	64	thickness:13	111	z_window_predicted:14
18	rx_roll	65	thickness:14	112	z_window_predicted:15
19	rx_pitch	66	thickness:15	113	PhiD
20	rx_yaw	67	thickness:16	114	PhiM
21	nlayers	68	thickness:17	115	PhiC
22	conductivity:1	69	thickness:18	116	PhiT
23	conductivity:2	70	thickness:19	117	PhiG
24	conductivity:3	71	thickness:20	118	PhiS
25	conductivity:4	72	thickness:21	119	Lambda
26	conductivity:5	73	thickness:22	120	AlphaC
27	conductivity:6	74	thickness:23	121	AlphaT
28	conductivity:7	75	thickness:24	122	AlphaG
29	conductivity:8	76	thickness:25	123	AlphaS
30	conductivity:9	77	thickness:26	124	Iterations
31	conductivity:10	78	thickness:27	125	Carriage return
32	conductivity:11	79	thickness:28		
33	conductivity:12	80	thickness:29		
34	conductivity:13	81	x_primary_predicted		
35	conductivity:14	82	x_window_predicted:1		
36	conductivity:15	83	x_window_predicted:2		
37	conductivity:16	84	x_window_predicted:3		
38	conductivity:17	85	x_window_predicted:4		
39	conductivity:18	86	x_window_predicted:5		
40	conductivity:19	87	x_window_predicted:6		
41	conductivity:20	88	x_window_predicted:7		
42	conductivity:21	89	x_window_predicted:8		
43	conductivity:22	90	x_window_predicted:9		
44	conductivity:23	91	x_window_predicted:10		
45	conductivity:24	92	x_window_predicted:11		
46	conductivity:25	93	x_window_predicted:12		
47	conductivity:26	94	x_window_predicted:13		

Appendix 4 Technical specifications of map projections

Projection Name:	Map Grid of Australia, Zone 51
Units:	Metres
Datum:	Geocentric Datum of Australia 1994 (GDA94)
Epoch:	1994.0
Ellipsoid:	GRS80
Semi-major axis (a):	6 378 160.0 metres
Inverse flattening (1/f):	298.25
Central meridian	123°00’00’’
False Easting:	500 000 metres
False Northing:	10 000 000 metres

Appendix 5 Conductivity logging

The following is Summarised from the GA internal report *"Logistics report for down-hole conductivity logging in the Paterson AEM Survey area, Western Australia, September 2008"* (Sorensen, 2008).

A5.1 Method

Induction conductivity logging tools measure the electrical conductivity of the material surrounding the borehole and provide a detailed indication of changes in conductivity with depth. Induction conductivity logging tools permit measurements of the electrical conductivity of the ground outside PVC cased boreholes generally without being sensitive to the presence of usually more conductive borehole fluid within the casing. Induction conductivity logging tools are capable of making reliable scientific measurements, however, their method of use has not been standardised. The following sections outline the method that was used in this data acquisition (Sorensen and Lane, 2007b).

The induction conductivity logging tool works in a similar way to ground or airborne electromagnetic systems. A small transmitter coil in the probe creates a primary magnetic field which gives rise to an electrical field in the materials surrounding the borehole. This electrical field creates eddy currents within the material, the strength of which depends on the conductivity of the material. These eddy currents then create a magnetic field which is measured with a receiver coil within the probe. **Figure A1** shows the principles of operation.

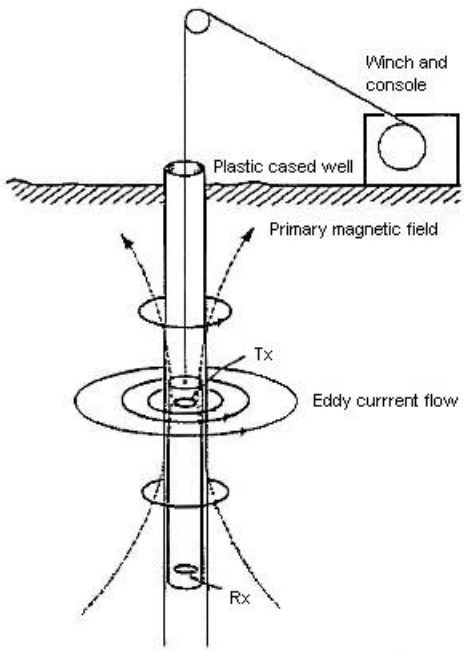

Figure A1: *The principle of operation of inductive conductivity borehole logging tool, from McNeill (1990).*

The geophysical logging equipment used on the fieldtrip was rented from Auslog Pty Ltd. The following equipment was used:

- Induction conductivity probe (HI327F serial no S500);

- Winch;
- Logging matrix console; and,
- Laptop with logging software (WellVision).

The location and elevation of each borehole was established using a Garmin GPS 60CSX. The standing water level was measured using a tape measure or a water level indicator when available. The height of the casing was measured using a tape measure.

Before lowering the conductivity probe, the condition of each hole was tested by running a dummy probe down and up the hole. If the dummy probe did not descend to the completion depth of the hole, the subsequent run with the conductivity induction tool was only carried out to the depth reached by the dummy probe.

Before calibration and data acquisition the temperature of the conductivity tool was stabilised. This was achieved by leaving the tool in the borehole at ~30m depth for 10-15 min.

Three calibration rings were provided with the induction conductivity logging tool: 100; 300; and, 500 mS/m. Calibration was always carried out before and after logging each borehole.

After temperature stabilisation of the instrument, calibration was carried out using the three calibration rings. The same procedures were adopted for each known calibration value; the probe was moved away from any metal and held in the air. To ensure that the probe was in a similar position while each calibration was performed, the probe was rested on the shoulder of one of the field party members as recommended by Auslog Pty Ltd. This procedure was then repeated for the other two calibration points.

Upon the completion of the tool calibration the temperature was again stabilised at 30 m depth for approximately 10 min. Prior to measuring the tool was positioned at a zero level, defined as the point at which the 'neck' of the probe (the point at which the end of the cable connector meets the probe) was level with the surface of the ground. While measuring, the logging speed was kept between 3-7 m/min, but was mainly between 5 and 7m/min. The details of the measuring procedures used for each bore were recorded on field logging sheets provided later in this appendix.

All holes were logged at least twice; once as the tool descended, and a second time as the tool ascended. On the completion of the upwards run, the two conductivity logs were overlain to ensure that repeatability was obtained. In a number of cases a minor discrepancy between the two logs existed, and additional runs with the tool were performed until the logs were consistent. In all cases consistency was observed after 1-2 additional logs were measured.

After each hole was logged the probe was recalibrated using the same procedures that were used in the pre-logging calibration. This was done to ensure a calibration of the probe was in the same state as when actually measuring in the borehole. It was then possible to compare pre- and post-logging calibrations and decide on which one was the most appropriate one to apply to the data in the processing step. In most of the cases the post-logging calibration seemed to be the most suitable as the conductivity tool was calibrated in a state as close as possible to borehole conditions.

A5.2 Results

After logging the 19 boreholes, the first hole logged (THRP161B) was re-logged. This was to ensure repeatability of the instrument over the 10 days it was used. Comparison of the repeat log and the original log (**Figure A2**) shows very little variation between the logs, indicating good repeatability.

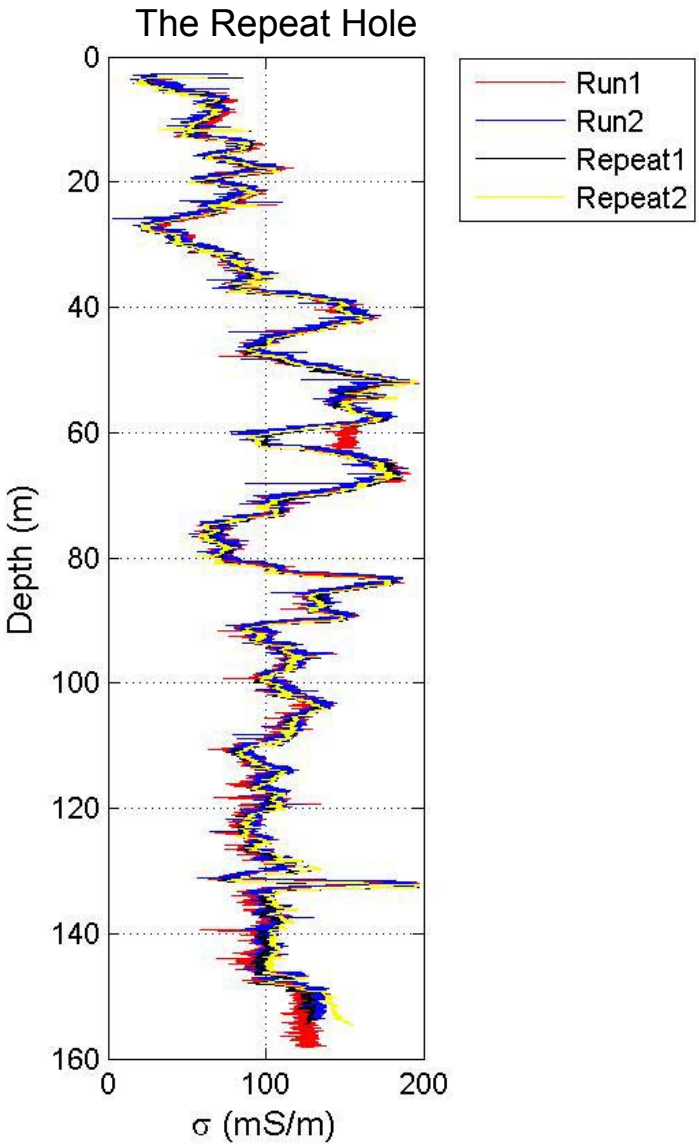

Figure A2: *Comparison of logs from the repeat hole, from the beginning and end of field trip. Run1 and Run2 were acquired at the beginning of the trip, and Repeat1 and Repeat2 were acquired at the end of the field trip.*

Figure A3 shows each of the 14 of the non confidential conductivity logs. Multiple runs at each hole are displayed. These plots show conductivity with depth, filtered with a median filter and then by moving average filter (both with filter width of between 5 and 31 points). The raw conductivity logs are not included in this report.

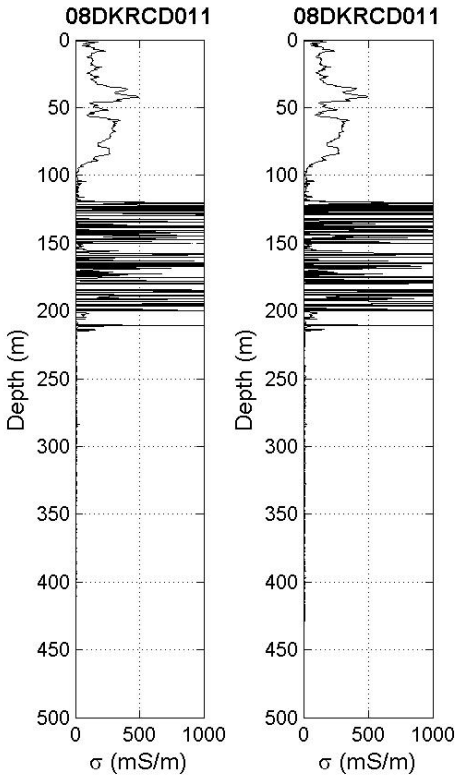
08DKRCD011
08DKRCD011
Depth (m)
σ (mS/m)
0
50
100
150
200
250
300
350
400
450
500
0
500
1000

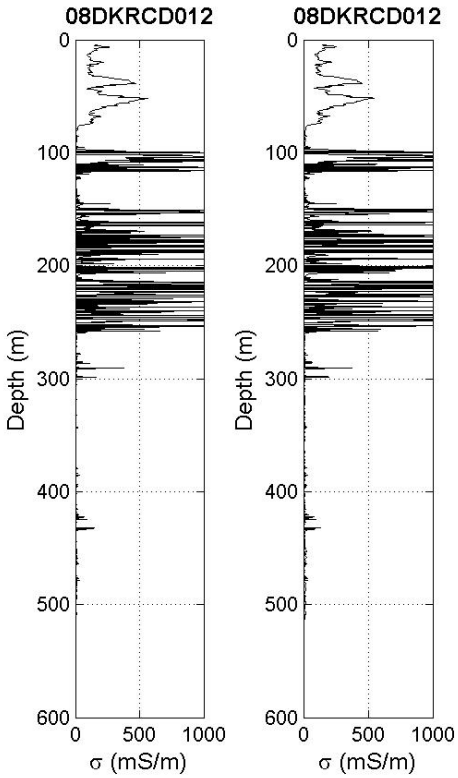
08DKRCD012
08DKRCD012
Depth (m)
σ (mS/m)
0
100
200
300
400
500
600
0
500
1000

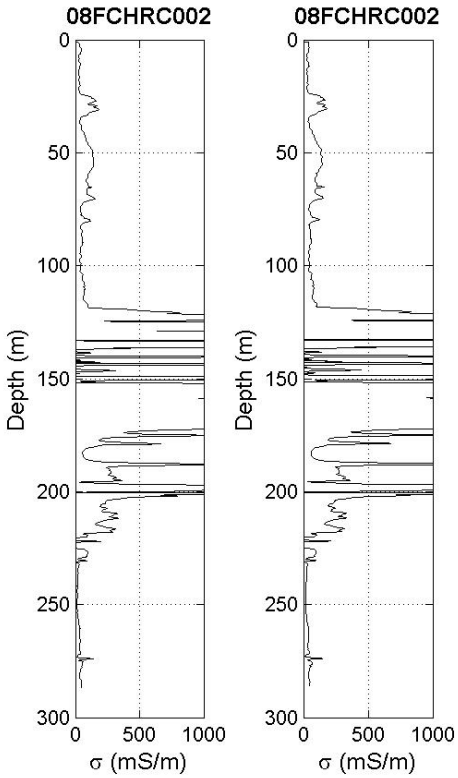
08FCHRC002
08FCHRC002
Depth (m)
σ (mS/m)
0
50
100
150
200
250
300
0
500
1000

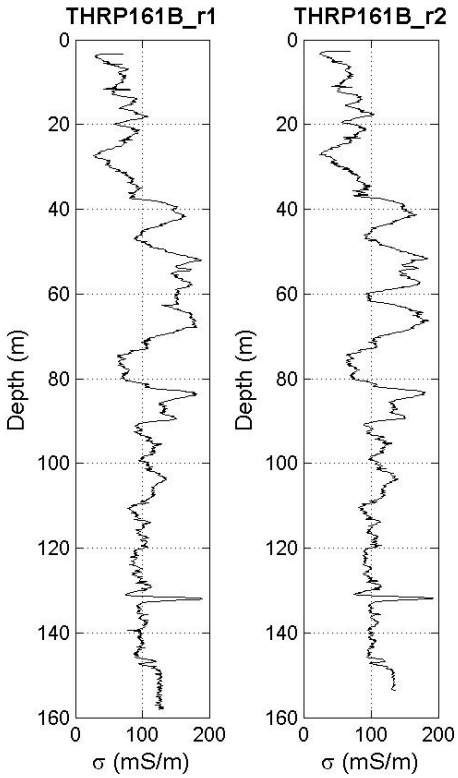
THRP161B_r1
THRP161B_r2
Depth (m)
σ (mS/m)
0
20
40
60
80
100
120
140
160
0
100
200

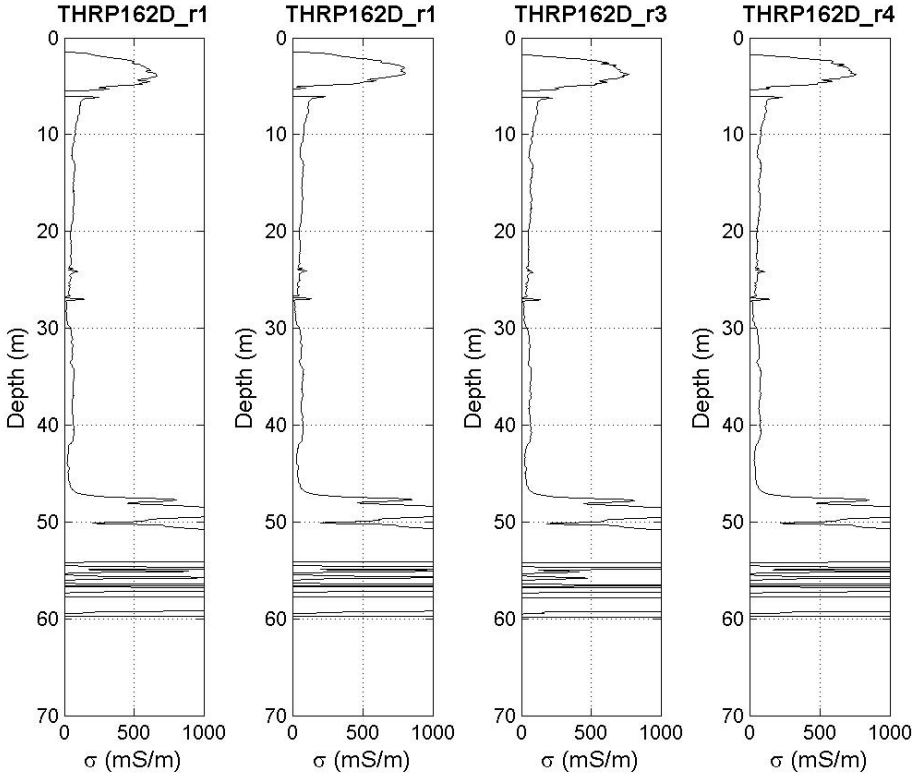
THRP162D_r1
THRP162D_r1
THRP162D_r3
THRP162D_r4
Depth (m)
0
10
20
30
40
50
60
70
0
500
1000
σ (mS/m)

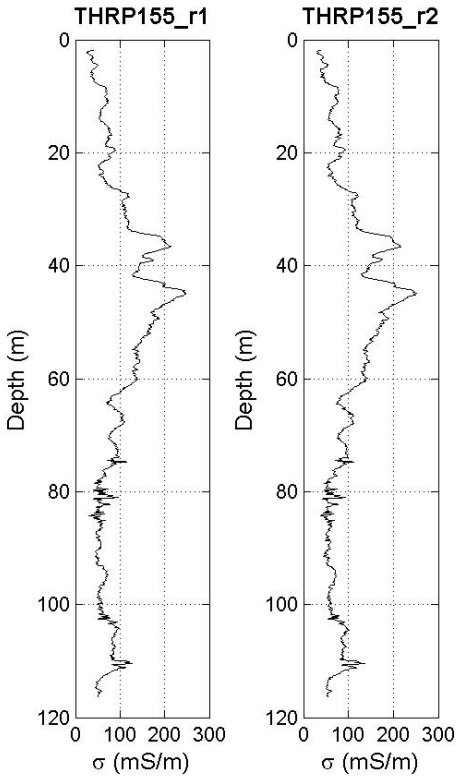
THRP155_r1
THRP155_r2
Depth (m)
σ (mS/m)
0
20
40
60
80
100
120
0 100 200 300

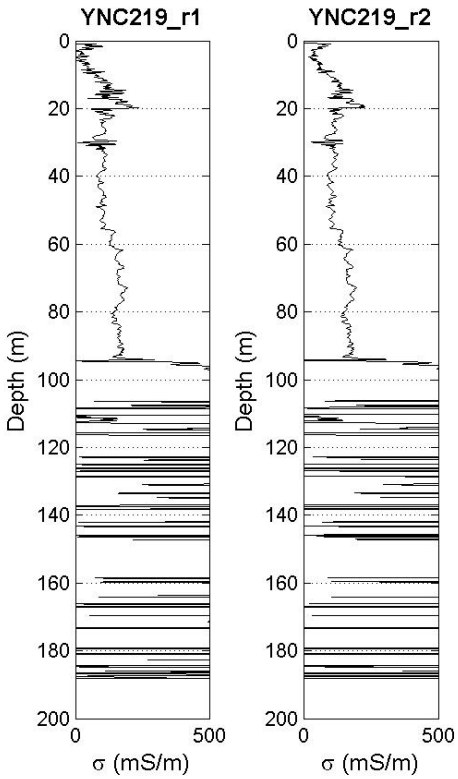
YNC219_r1
YNC219_r2
Depth (m)
σ (mS/m)
0
20
40
60
80
100
120
140
160
180
200
0 500

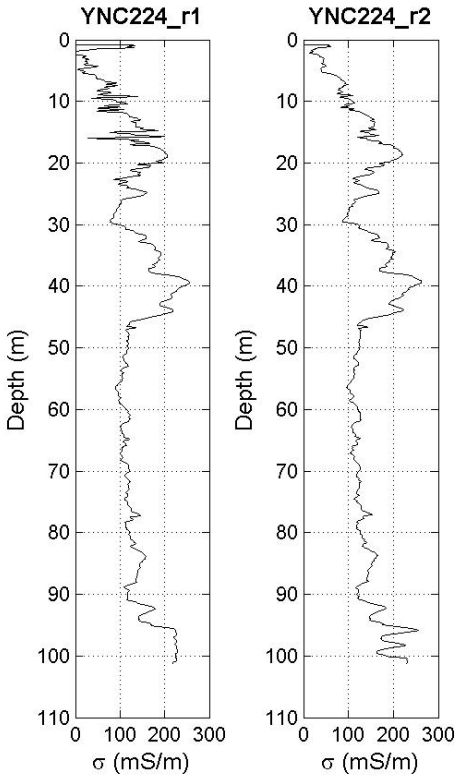
YNC224_r1
YNC224_r2
Depth (m)
σ (mS/m)
0
10
20
30
40
50
60
70
80
90
100
110
0
100
200
300

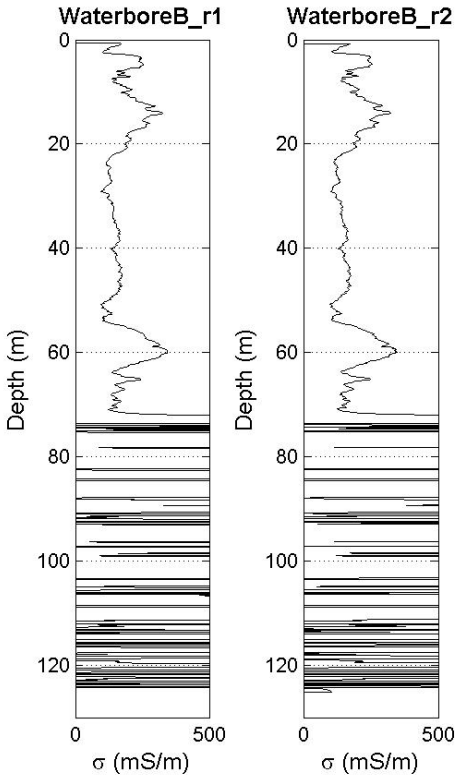
WaterboreB_r1
WaterboreB_r2
Depth (m)
0
20
40
60
80
100
120
0
500
σ (mS/m)

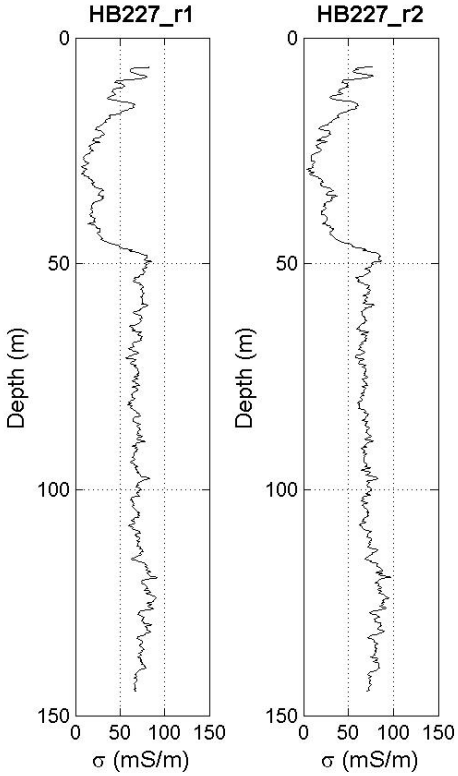
HB227_r1
HB227_r2
Depth (m)
0
50
100
150
0 50 100 150
σ (mS/m)

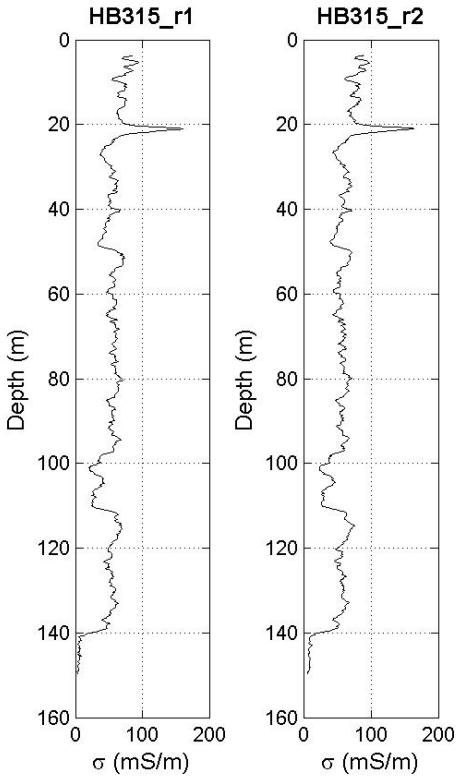
HB315_r1
HB315_r2
Depth (m)
σ (mS/m)
0
20
40
60
80
100
120
140
160
0
100
200

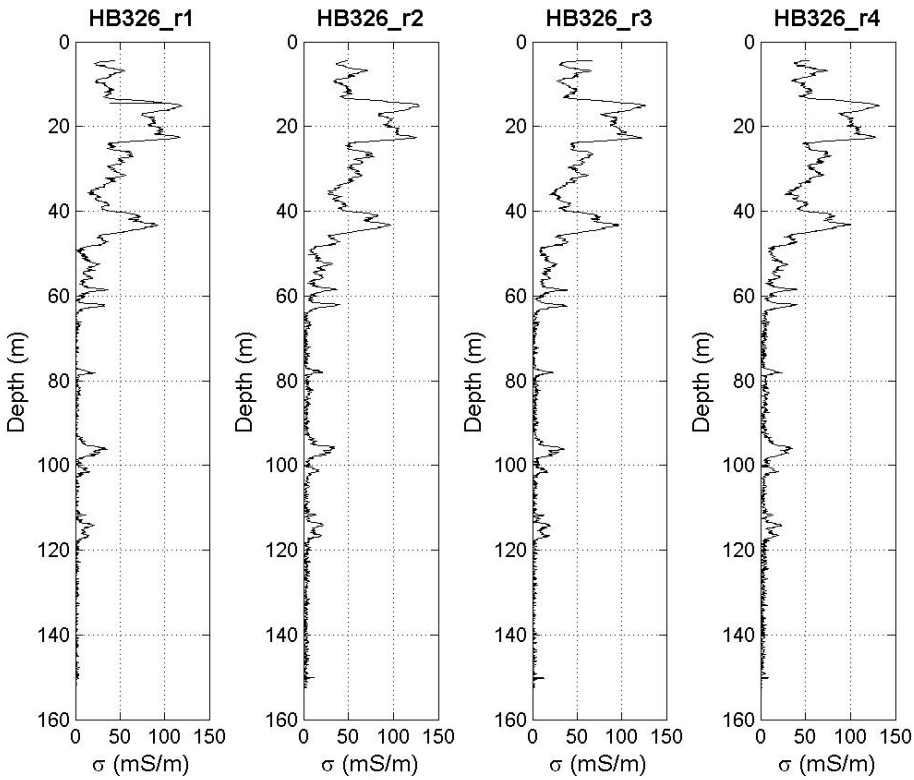
HB326_r1
HB326_r2
HB326_r3
HB326_r4
Depth (m)
σ (mS/m)
0
20
40
60
80
100
120
140
160
0
50
100
150

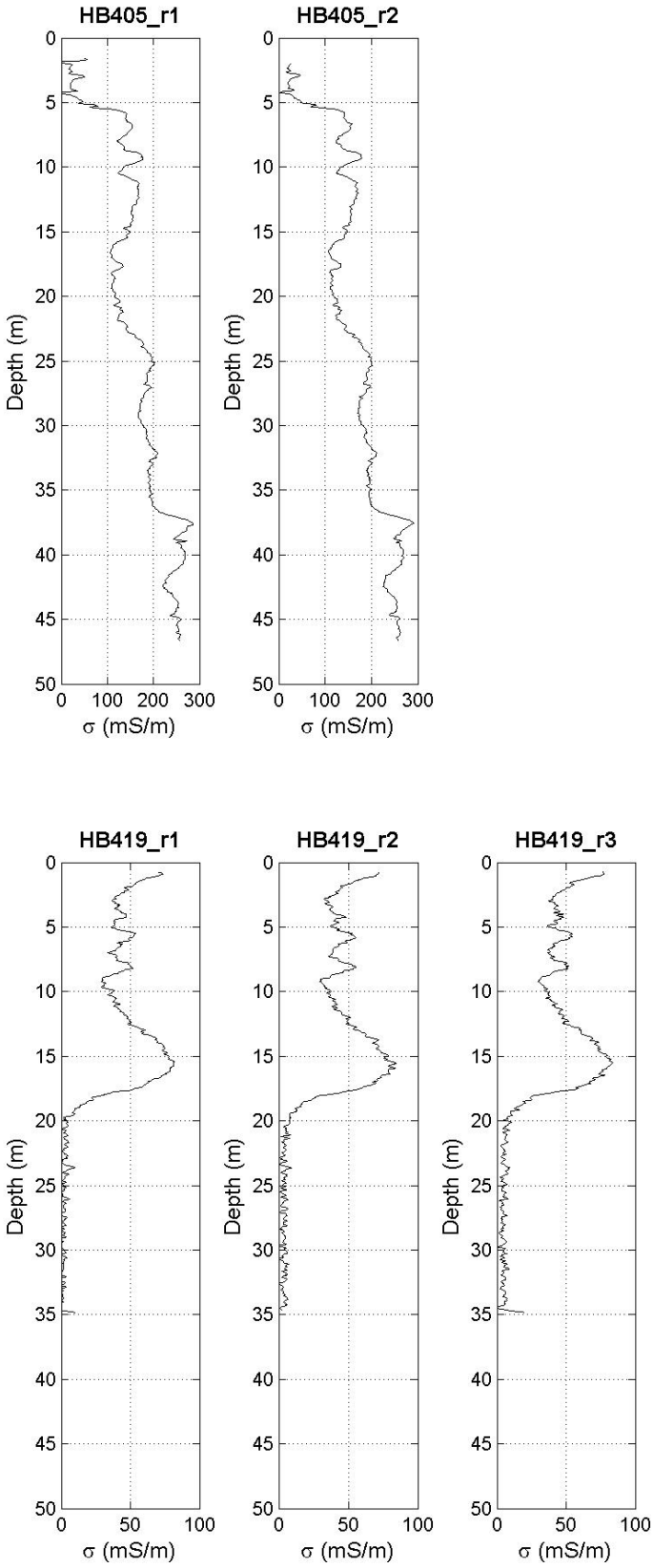

Figure A3: *The 14 publicly available conductivity logs, showing the repeat passes acquired for each log.*

A5.3 Field sheets

Field sheets were filled in for each of the conductivity logs acquired during the 2008 field trip to the Paterson Region; an example is provided below (**Table A1**).

Table A1: Field sheets acquired for conductivity logs.

			Method (e.g. tape, GPS etc.)	
Location/Site name	08DKRCD011			
Easting	51 K 0348403		GPS	
Northing	7657601		GPS	
Map Datum	WGS84		GPS	
Projection				
Surface elevation	811ft		GPS	
Height of casing				
Water level	3.72m			
Depth of hole	428m			
Drill method	RC + DD			
Casing info	**Type**	**Size**		**Depth interval**
	PVC	40mm		428m

Probe information

Type of probe	**Name**	**Serial number**
Conductivity	A085	S500

Log information (08DKRCD011)

Type of log	Induction Conductivity			
Name of operator(s)	Camilla Sorensen (Geoscience Australia)			
Run #	**1**	**2**	**3**	**4**
Date	30/08/2008	30/08/2008		
Time	9.45	11		
Logging speed (m/min)	6 m/min	7 m/min		
Temperature stabilised?	Probe left at 30m for 10min	Yes		
Repeatability?	Yes reasonably			
Irregularities	None	None		
Weather info	Hot	Hot		
Units of measurement	mS/m	mS/m		